



School of Chemistry

Porous Carbon Supercapacitors: Development, Applications
and Future Materials

Markus Standen

**This thesis is submitted in partial fulfilment of the
requirements for the Honours Degree of MSci at the
University of Bristol, 2021**

Supervisor: Paul May

Second Assessor: Neil Fox

Third Assessor: Neil Allan

Physical and Theoretical Group

Abstract

Supercapacitors are a form of charge storage device that operate in a similar way to conventional capacitors, that is they store energy in the form of charges which accumulate on two oppositely charged electrodes as a potential difference is applied across the device. To be exact, charge is stored in an electrical double layer which forms between a porous electrode and an electrolyte solution, though this exact mechanism is complex and uncertain. Supercapacitor devices can be charged and discharged very quickly, can be cycled many times (over 10,000) with minimal deterioration and have appreciably high energy storage, all of which allow them to be used for a wide variety of applications. They effectively bridge the gap between high-power conventional capacitors and high-energy electrochemical cells (batteries).

In this literature review, the development, applications and possible future material types of porous carbon supercapacitors are discussed. First, the theoretical mechanism of charge storage is explored. For planar supercapacitors, the modern theories of the electric double layer formation are well accepted, but the intricacies of the networks in porous supercapacitors bring complications and phenomena that are of continued discussion among researchers. Some conclusions of the storage mechanism in porous supercapacitors can be made, and emphasis on the need for large surface areas, increased micro-porosity (pore diameter < 2 nm) and meso-porosity (pore diameter between 2-50 nm) are given. This leads onto discussions of the key characteristics of successful supercapacitors, such as performance, reliability, safety, and cost, and how in particular the performance metrics of supercapacitors are typically evaluated through cyclic voltammetry and galvanostatic charge-discharge measurements.

The overall cell design of supercapacitors and how these relate to their wide-ranging applications are then discussed in detail. Supercapacitors can be divided by their scale (large- or small- scale applications) and their focus on high power versus high energy. Applications of supercapacitors range from instantaneous backup power for small electronics components, such as memory cards, to efficient energy storage and charge-discharge cycle devices for use in kinetic-energy-recovery systems that are popularly used in hybrid vehicles.

The historical developments and advantages of carbon-based supercapacitors are then discussed in detail. Examples of graphitic carbon devices, ranging from the historic and simple to produce activated carbons to the more exotic porous templated carbons and carbon nanotubes, are presented. Typically, these devices have large surface areas, highly tuneable pore-size distributions and are relatively cheap and easy to manufacture. Alternatively, boron-doped diamond is also presented as a recently developed carbon supercapacitor material, with unique properties such as high chemical stability that allows for a wider applicable voltage range.

Prototypes of these diamond-based devices are presented which display advantages and disadvantages when compared with graphitic carbons, namely they have very high power outputs but very low energy-storage abilities. Lastly, potential avenues for the future development of diamond supercapacitors are discussed.

Table of Contents

Abstract	2
1 - Acknowledgements	4
2 – Important abbreviations	5
3 – Introduction	6
4 – Fundamentals of electrochemical capacitors	7
4.1 – Conventional capacitors.....	7
4.2 – Electrochemical capacitors	7
4.3 - EDL formation in porous materials	9
4.4 – Pseudocapacitance	11
5 – Operation and measurement of supercapacitors	12
5.1 – Key supercapacitor characteristics.....	12
5.2 – Common electrochemical measurements	13
5.2.1 - Cyclic voltammetry	13
5.2.2 - Galvanostatic charge-discharge	15
5.3 – Supercapacitor cell design and applications	16
5.4 – Supercapacitor electrolytes.....	19
6 – Developments in carbon-based supercapacitors	20
6.1 – Activated carbon powders	20
6.2 – Activated carbon fibres	22
6.3 – Carbon Aerogels	23
6.4 - Porous templated carbon	24
6.5 – Carbon nanotubes	29
6.6 – Summary of graphitic carbon supercapacitor electrodes	32
7 – Diamond-based supercapacitors	33
7.1 – Suitability of diamond for supercapacitor use.....	33
7.2 – Reports of diamond supercapacitors	34
7.3 – Summary of diamond supercapacitor electrodes	38
8 – Conclusions	39
9 – References	40

1 - Acknowledgements

I would like to thank my supervisors Paul May and Neil Fox for their helpful discussions and guidance during the writing of this review.

2 – Important abbreviations

EDL	Electrical Double Layer
EDLC	Electrical Double Layer Capacitor
EDC	Electrical Double Cylinder
EDCC	Electrical Double Cylinder Capacitor
EWCC	Electrical Wire-in Cylinder Capacitor
CV	Cyclic Voltammetry
GCD	Galvanostatic Charge-Discharge
ESR	Equivalent Series Resistance
AC	Activated Carbon
ACF	Activated Carbon Fibre
CAG	Carbon Aerogel
SEM	Scanning Electron Microscopy
CNT	Carbon Nanotube
SWCNT	Single-Walled Carbon Nanotube
MWCNT	Multi-Walled Carbon Nanotube
VACNT	Vertically Aligned Carbon Nanotube
CVD	Chemical Vapour Deposition
BDD	Boron-Doped Diamond

3 – Introduction

Supercapacitors (also called ultracapacitors or simply electrochemical capacitors) are a form of charge-storage device commonly used in consumer electronics, public transport and heavy industry.¹ Much like a ‘normal’ capacitor, a supercapacitor functions by storing charge at the surface of a conducting plate, and in doing so, it stores energy in the electric field generated between two oppositely charged planar regions. Whereas a parallel-plate capacitor employs two parallel plates of conducting metal, between which a dielectric material is placed, a superconductor is more akin to an electrochemical cell: a pair of oppositely charged electrodes are placed within an electrolyte solution and store energy when an electrical double layer of solvated ions forms on the surfaces of the electrodes.²

Supercapacitors are characterised by having very high specific power values, i.e., being able to deliver large amounts of energy in short periods of time. However, they often suffer from having lower specific energy values, meaning they cannot store very large amounts of energy in comparison to other charge-storage devices, such as conventional batteries.¹ As such, supercapacitors were historically, and still are, largely used as an auxiliary power source in tandem with high-energy storage devices like batteries. Such an arrangement is useful for electronics and computer components that have fluctuating energy demands susceptible to sudden losses of power.^{1,3}

Crucial to the effective design and operation of a supercapacitor is the task of creating electrodes with extremely large surface areas. As the charge-storage capability of the device is based upon the electrostatic interactions between electrolyte and electrode surface, the greater the effective surface area of the electrodes, the greater the supercapacitor. Therefore, the use of porous electrodes has been the basis of supercapacitor design since their inception.^{1,3}

Perhaps the most exciting application of modern supercapacitors has been in electric / hybrid vehicle design, where their potential use is often seen as a solution to global energy demands among increasing efforts to combat climate change.⁴ Though the use of electric vehicles has become more widespread, arguably the largest drawback in comparison with petrol cars is excessive refuelling time. Compared with the few minutes it takes to refuel a petrol car, the ‘empty to full’ charging time of, for example, the 2018 Nissan Leaf⁵ is, at best 6 hours, using expensive 22 kW fast chargers (only typically accessible at public locations or petrol stations), and, at worst, 18 hours (using a plug-in-at-home charger). Whilst there are practical solutions to this issue and charging performance is often better when the batteries aren’t completely empty, the problem still remains, and the comparable ease and convenience of petrol vehicles is obvious.

If supercapacitors could be developed to have specific-energy storages comparable or better than modern battery technology, whilst retaining the fundamental feature of having high power density and fast charge/discharge rates, all while remaining safe, environmentally friendly and cost effective, they could be very effectively utilised as a replacement for (or in conjunction with) batteries in a wide variety of technological applications - fast-charging electric vehicles being just one of them.

This work will review carbon-based supercapacitors presented in literature, with an emphasis on the effectiveness of diamond as a material for supercapacitor construction and with a view towards continued research into diamond supercapacitors within the University of Bristol CVD Diamond Group.

4 – Fundamentals of electrochemical capacitors

4.1 – Conventional capacitors

As mentioned previously, a conventional capacitor is an electrical device which stores charge by applying a potential difference across two plates of conducting metal separated by a dielectric material. As the voltage is applied across the two plates, an electric field is generated across the dielectric layer which causes opposite charges to accumulate on either side and (ideally) remain even after the external power supply driving the potential difference has been switched off. The device can then be discharged to supply the stored energy to another electrical component. Figure 1 shows a schematic of a parallel plate capacitor.³ This effect is measured as capacitance (C), and is the ratio of the built-up electric charge (q) to the corresponding electric potential (V), and has units of farads, F. For a parallel-plate capacitor with plate surface area A , dielectric material constant ϵ_r , vacuum permittivity ϵ_0 , and separation of the two plates by distance d , the capacitance is given by:

$$C = \frac{\epsilon_r \epsilon_0 A}{d}. \quad (\text{Eq. 1})$$

Furthermore, the maximum energy (E) that can be stored by a parallel-plate capacitor is given by:

$$E = \frac{1}{2} CV^2. \quad (\text{Eq. 2})$$

Therefore, the key factors to consider when improving the design of conventional capacitors are maximising both the permittivity of the dielectric and the surface area of the parallel plates, minimising the distance between the plates, and maximising the voltage applicable across the capacitor device (all without causing the capacitor to breakdown and begin conducting charge across the dielectric).

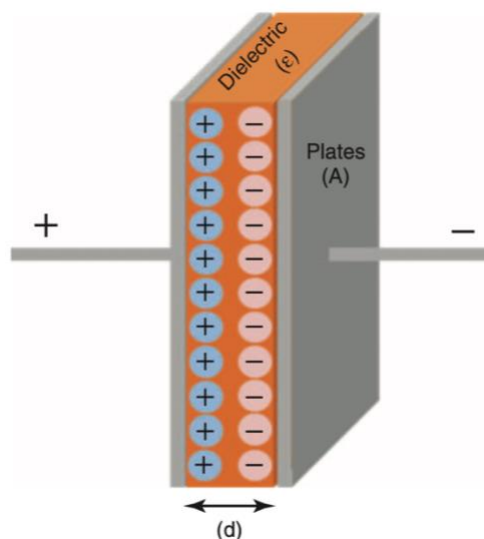


Figure 1: Schematic diagram of a parallel-plate capacitor, showing arrangement of charges across dielectric material.³

4.2 – Electrochemical capacitors

In contrast, electrochemical capacitors store charge in the static electric field generated by the formation of an electrical double layer (EDL) between electrical charges on the surface of a (porous) electrode and ionic charges dissolved as part of an electrolyte

solution. Figure 2 shows a schematic diagram of an electrical double layer capacitor (EDLC) with a porous carbon electrode together with the corresponding change in voltage across the interface.⁶ In this case, the water molecules on the solvated electrolyte ions serve as the dielectric medium which prevents charge transfer between the two oppositely charged surfaces.

Understanding of the mechanism which characterises the formation of the EDL has developed over time, and its application to supercapacitors is of continued investigation.⁶ Figure 3 displays the 3 discussed models for the EDL which describe the charge storage mechanism for supercapacitors.⁶

The EDL was first characterised by Hermann von Helmholtz, who originally theorised the concept in relation to the interface between oppositely charged media of colloidal particles. He theorised that a certain charge distribution would form (called the Helmholtz double layer), where two layers of opposite charge would form at the interface (between colloidal particles, or in this case, between the electrode and electrolyte), separated by dipoles of the electrolyte solvent.

However, the Helmholtz EDL does not account for other observed phenomena and behaviour of charge interfaces. The Gouy-Chapman EDL model considers the continuous distribution of both positively and negatively charged ions throughout the electrolyte phase, called the diffuse layer. The ion concentration can be characterised by the Maxwell-Boltzmann distribution, which allows for capacitance to vary with temperature and the nature of the ions in solution. Yet in circumstances where the EDL is highly charged, the original Helmholtz model appears to better characterise the system. The Stern model is effectively a combination of the Helmholtz and Gouy-Chapman model: it proposes that a compact layer (also called the Stern layer) exists closest to the electrode surface containing a dense layer of counterions, often hydrated by the solvent, which are adsorbed onto the electrode surface, while the diffuse layer (as described by the Gouy-Chapman model) continues beyond. Further additions by Grahame (which are often assumed incorporated with the Stern model) allow for the often-observed specific adsorption of ions (without hydration shells) onto the electrode surface and distinguishes this specifically adsorbed layer, the Inner Helmholtz Plane (IHP), from the distance of closest approach for the solvated ions, the Outer Helmholtz Plane (OHP).

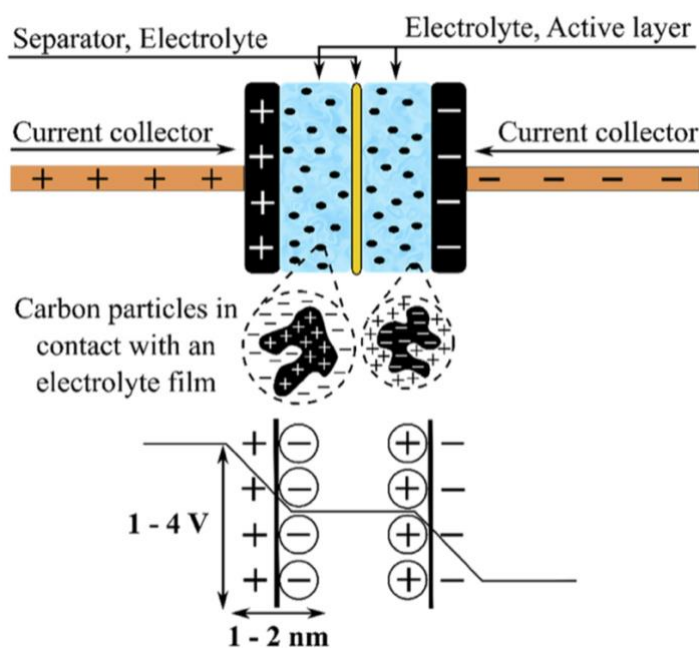


Figure 2: Schematic diagram of an EDLC with porous carbon electrodes (represented by black dots), demonstrating the EDL interface and the corresponding voltage changes across it.⁶

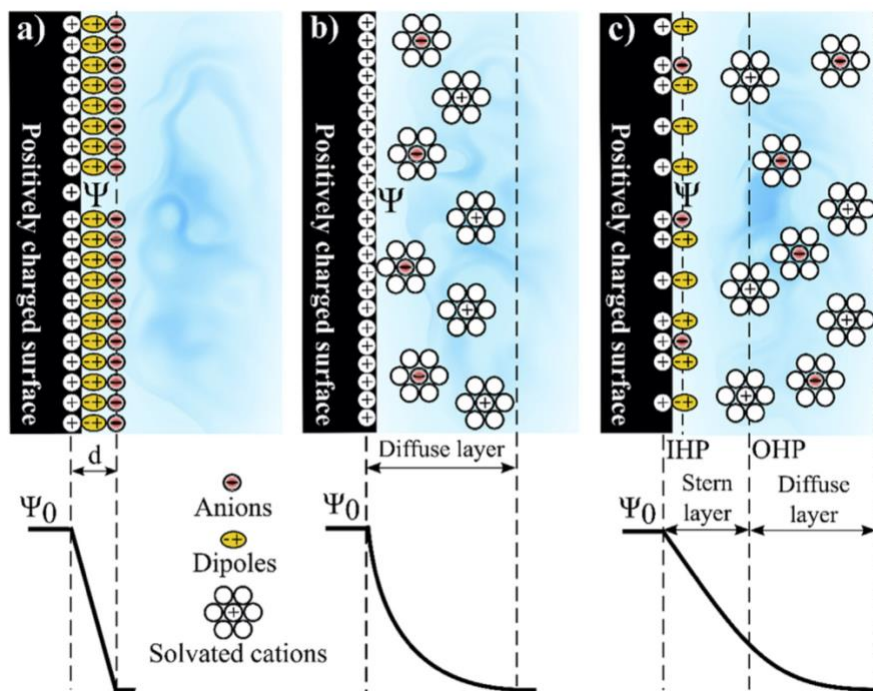


Figure 3: Diagrams showing the 3 developments in the EDL models for describing charge storage in supercapacitors: a) the Helmholtz model; b) the Gouy-Chapman model; c) the Stern model. Also shown are the changes in potential (Ψ) across the interface.⁶

So far, these models are physically comparable to the conventional parallel-plate capacitor model. Thus, by applying Eq. (1), the distance separating the two ‘plates’ is of the order of atomic distances, and the surface area (if the electrodes are porous and in full contact with the electrolyte solution) can be orders of magnitude larger than that of a rectangular plane, already demonstrating the greatly increased capacitive ability. Also, the total capacitance of the EDL (C_{EDL}) is related to the sum of the reciprocal values of the individual capacitance of the compact (C_H) and diffuse (C_{diff}) layers by:

$$\frac{1}{C_{EDL}} = \frac{1}{C_H} + \frac{1}{C_{diff}}. \quad (\text{Eq. 3})$$

However, the intricacies of the commonly used porous electrodes in supercapacitors result in experiments deviating from the standard parallel-plate assumption. The porous nature of such electrodes means that variations in shape, size and accessibility of the pores, will result in different exact mechanisms by which the EDL will form, and will certainly begin to deviate from that of a planar, parallel surface. Therefore, beyond the applied voltage, the nature of the electrolyte solution and the overall surface area, the factors which will affect the EDL formation and capacitance of an EDLC will include the wettability of the electrode surface by the electrolyte, the mass-transfer path of the electrolytes, and crucially, the size of the electrolytes in relation to the pore-size distribution of the electrode.

4.3 - EDL formation in porous materials

When classifying porous materials, the size distribution of pores is usually given in relation to three main categories: macropores (above 50 nm), mesopores (between 50 nm and 2 nm) and micropores (below 2 nm).⁷ Pores are further distinguished by their interconnectivity and availability to the surroundings, and also by their shape, generally either cylindrical or slit-shaped.⁷ Historically, it was assumed that the smallest pores, micropores and sub-micropores, did not contribute to the formation of the EDL and therefore

had no capacitive effect. Though the average sizes of the electrolyte ions used are usually of the order of 0.1 - 0.4 nm (e.g., commonly used quaternary ammonium salts such as TEABF₄ have ionic radii $r(\text{TEA}^+) = 0.343$ nm, $r(\text{BF}_4^-) = 0.229$ nm),⁸ when solvated, the size of these ions exceed the size of the pores, and it was assumed that these ions need to be fully solvated to participate in EDL capacitance. However, experimental results revealed anomalous increases in capacitance using largely microporous electrodes and it was concluded that partially or even entirely desolvated ions could enter the sub-nm micropores and contribute to the capacitance of the system.⁹

The aforementioned EDL mechanisms are not applicable in this situation, as there is insufficient room for the formation of both compact and diffuse layers. The appropriate mechanisms by which to describe these highly complex porous materials is of continued discussion amongst researchers, and some very effective models have been proposed in recent years.⁶ One of the earliest such models was proposed by Huang et al., in which the mesopores and micropores of a porous carbon electrode were assumed to be cylindrical.¹⁰ For cylindrical mesopores, the space within is considered large enough to allow for fully solvated counterions, essentially akin to an EDLC model but cylindrical. Hence, these are called Electrical Double Cylinder Capacitors (EDCC), with capacitance (C_{EDCC}) values given by:

$$C_{\text{EDCC}} = \frac{2\pi\epsilon_r\epsilon_0 L}{\ln(b/a)} \quad \text{or} \quad \frac{C_{\text{EDCC}}}{A} = \frac{\epsilon_r\epsilon_0}{b\ln(b/(b-d))}, \quad (\text{Eq. 4})$$

where L is the length of the pore, a is the radius of the inner cylinder and b the outer cylinder, with $(b - a)$ is equal to d , the effective thickness of the electric double layer (i.e. the Debye length, as with the EDLC models). For the cylindrical micropores, as before, it is assumed that there is insufficient space to accommodate an EDL (or here even an EDC), meaning counterions (either solvated or desolvated, but small enough to fit) may enter the pores one at a time, and line up to form what is called an Electrical Wire-in-Cylinder Capacitor (EWCC), with capacitance (C_{EWCC}) values given by:

$$\frac{C_{\text{EWCC}}}{A} = \frac{\epsilon_r\epsilon_0}{b\ln(b/a_0)}, \quad (\text{Eq. 5})$$

where a_0 is the effective size (or extent of electron density) of the counterions. Figure 4 shows schematic diagrams of the EDCC and EWCC models in mesopores and micropores, respectively.¹⁰

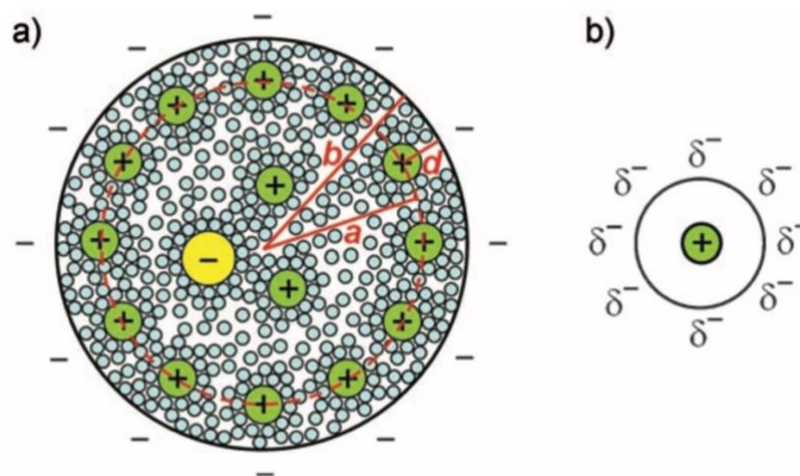


Figure 4: Schematic diagrams showing cross sections of: a) a negatively charged mesoporous electrode with positive counterions forming an EDCC with inner radius a and outer radius b (difference d), and b) a negatively charged microporous electrode with single positive counterions forming an EWCC with pore radius b and counterion radius a_0 .¹⁰

These models were fitted to the previously anomalous results and were found to be in good agreement. It was concluded that both mesopores and micropores contributed to the capacitance of porous electrodes, and that they should be approximated as cylinders, using a combination of the EDCC and EWCC models. Further discussion and investigation has continued to develop the understanding of 'EDLC-like' capacitance in porous electrodes, with other models being developed which include: other ways of describing the pores of the electrodes as both slits and cylinders; highlighting the difference in utility of micropores for active sites for accommodating ions with meso- and macro-pores for rapid ion transport upon changing polarisation; and noting the variability of the material dielectric constant in different circumstances.

However, it is sufficient to note that the pore size-distribution of the porous electrode in relation to the nature, size and wettability of the electrolyte solution with the electrode, is critical to controlling the capacitive and energy storage ability of an 'EDLC-like' supercapacitor. Therefore, materials with easily tuneable pore size distributions are optimal for use in supercapacitors.

4.4 – Pseudocapacitance

Though not the focus of this review, it is worth noting the other, but hardly insignificant, mechanism by which supercapacitance is achieved besides the 'EDL-like' capacitance (including EDCC/ECWW, etc. mechanisms), known as pseudocapacitance. Pseudocapacitance is caused by very fast and reversible redox reactions (termed 'faradaic' reactions between specifically adsorbed electrolyte ions and the electrode surface.² As opposed to EDL capacitance, which is electrostatic in nature, pseudocapacitance involves electron transfer at the electrode surface, essentially a reaction (though strictly not chemically). This effect occurs when desolvated ions pass through the EDL and specifically adsorb to the electrode, meaning this effect always occurs alongside the electrostatic EDL-like effect.⁶ However, because the adsorbed ions are desolvated and therefore smaller and closer to the electrode, the capacitance and specific energy achievable due to pseudocapacitance can be orders of magnitude greater than that due to EDL capacitance alone.⁶

Pseudocapacitors also require different electrode materials to produce effective active sites for charge transfer, including transition-metal oxides such as ruthenium oxide (RuO_2 , which is very popular), manganese oxide (MnO_2) and vanadium nitride (VN), as well as polymers like polyaniline or generally materials with oxygen or nitrogen containing functional groups. Though these pseudo-capacitance-active materials can be specifically doped within conductive carbon electrodes, the metal oxides, in particular, are expensive and difficult to manufacture.^{2,6} Furthermore, the process of specific adsorption through the EDL can sometimes result in a slower charge-discharge process compared to the electrostatic EDL effect, which can result in poorer specific power and cycling stability problems.

As mentioned previously, the development of electrodes designed for optimal pseudocapacitance is not discussed in this report: carbon materials are used primarily for EDLC electrodes (hence as would diamond), and though pseudocapacitance is an important effect, these two areas of research are relatively independent. This is especially so, as supercapacitors are often designed to be hybrids (also called asymmetric supercapacitors), where one electrode is primarily an EDLC and the other is a faradaic pseudocapacitor.⁶

5 – Operation and measurement of supercapacitors

5.1 – Key supercapacitor characteristics

The supercapacitor industry, as expected with any battery or energy-storage industry, is driven by many factors but fundamentally these are performance, safety and cost. Whilst safety and cost may be easy to measure, the difficulty in measuring and evaluating the performance of supercapacitors is heavily linked to the difficulty in characterising the previously discussed mechanisms of charge storage. The porous nature of the electrodes and the presence of both ideal EDL-capacitance and pseudocapacitance complicates the measurement and analysis of supercapacitors and makes it difficult to definitively state capacitance, power and energy storage values. Furthermore, a review paper by da Silva et al. (2020) and literature surveys referenced within suggest many articles presenting novel supercapacitors use widely varying experimental protocols to measure their devices and often misapply equations to calculate specific energy-storage and power, in particular.⁶ This review is not intended to consider some of these issues and will instead focus on the broadly used methods for characterising supercapacitors and will present promising literature results as reported in the literature.

Regardless, the most important criteria for evaluating supercapacitors are the following:²

- 1) **Power density**, the deliverable power output of the supercapacitor per unit mass. As before, high power density is the primary advantage of supercapacitors over batteries, and so this value must be substantially greater than any comparable battery technology.
- 2) **Energy density**, the total amount of energy that can be stored in the supercapacitor per unit mass. Supercapacitors will almost always perform poorly compared to batteries on this metric but must still be acceptably high ($>10 \text{ W h kg}^{-1}$ according to Zhang et al., 2009)².
- 3) **Cyclability / lifespan**, how many charging cycles (at a given temperature) the supercapacitor can perform before it begins to decrease in total power or energy output (and therefore how long the device lasts). This is another value that should be much greater than any comparable batteries.
- 4) **Charging time**, how quickly the device can charge and discharge. This value will be proportional to the power and energy density and should be of the order of a few seconds.
- 5) **Self-discharging times**, how quickly the device will leak charge when not active. Ideally this effect will be minimal.
- 6) **Voltage and temperature operating windows**, the range of voltage and temperature values within which the supercapacitor can safely and effectively operate. These parameters have a crucial impact on safety, reliability and usability within varying contexts. Ideally these ranges are very broad, but most importantly the devices should work at common temperatures and voltages, such as room temperature and mains voltage.
- 7) **Safety**, including factors such as reliability and user safety (which will depend heavily on the operating windows) as well as environmental considerations (waste material and recyclability).
- 8) **Cost**, including scalability, ease of production and the rarity of certain materials.

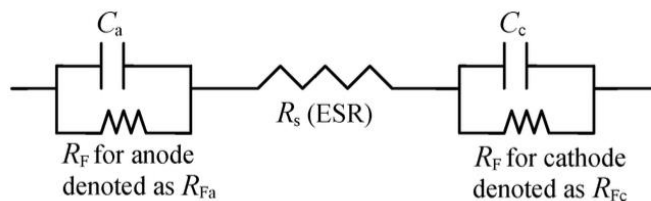


Figure 5: Equivalent RC circuit diagram of a supercapacitor, with each electrode having unique resistance and capacitance values, with an equivalent series resistance between the two.²

Figure 5 shows a two-electrode supercapacitor in an RC circuit (Resistor-Capacitor) representation.² As an EDL is formed at both electrodes in a supercapacitor, each electrode is effectively its own capacitor, with unique capacitance and resistance (responsible for self-discharge) values C_a and R_{Fa} for the anode and C_c and R_{Fc} for the cathode. Also present is an Equivalent Series Resistance (ESR) between the two electrodes, denoted R_s . As per Eq. (3), the capacitance values for the two electrodes sum in a reciprocal manner to give the total capacitance, C_T , which in turn can be used to calculate the maximum energy stored (E_{max}) and the maximum deliverable power (P_{max}) as per the following equations:

$$E_{max} = \frac{1}{2} C_T V^2, \quad (\text{Eq. 6})$$

$$P_{max} = \frac{V^2}{4R_s}, \quad (\text{Eq. 7})$$

where V is the cell voltage. Eq. (6) and Eq. (7) demonstrate the 3 key factors which indicate good supercapacitor performance: a high capacitance, which as previously discussed depends primarily on the electrode design (surface area, material and pore size); a high cell voltage, which depends on the thermodynamic stability of the electrolyte solution; and a minimum ESR, which depends on the overall resistances in the various structural elements of the device (between the current collector and the electrodes, within the electrolyte solution due to mass transfer resistance, etc.).

5.2 – Common electrochemical measurements

There are a wide variety of measurement techniques employed to characterise supercapacitors and determine the important values previously discussed. Most research papers on the topic include measurements on characterising the physical properties of the electrode surfaces such as surface area and imaging techniques, as well as electrochemical measurements to arrive at capacitance, power and energy values. However, there are two very commonly used electrochemical techniques which are worth noting: Cyclic Voltammetry (CV) and Galvanostatic Charge-Discharge (GCD) measurements.

5.2.1 - Cyclic voltammetry

CV measurements involve applying a varying electrode potential across the supercapacitor device fitted with a reference electrode and measuring the current response. Some methods require separate measurements for each device electrode with the reference electrode while others do not.¹¹ As the name suggests, this varying electrode potential is cycled (i.e., ramped up and down) across the working potential window within which the electrolyte solution is stable, and so simulates the charging and discharging processes of the supercapacitor device. This measurement technique is therefore extremely useful for evaluating supercapacitors because it not only can be used to calculate capacitance and therefore energy and power values, but crucially as a function of the voltage scan rate, over

the device potential operating window. If cycled repeatedly as a function of cycle number, this procedure indicates the cyclability and lifespan of the device. The capacitance dependence upon scan rate is particularly important as, in the case of porous supercapacitors, the reduced ion transport and the ESR of the porous electrodes is expected to result in worsening capacitance with increased scan rate.

Assuming a linear scan rate ($V = V_0 \pm vt$), with cell voltage V (initial voltage V_0 , voltage range $\Delta V = V - V_0$, units V), scan rate v ($V s^{-1}$) and time t (s), a model for the CV profiles of an ideal supercapacitor is given by:¹²

$$I = Cv \left[1 - \exp\left(\frac{-\Delta V}{CvR_s}\right) \right], \quad (\text{Eq. 8})$$

where I is the current (A), C is the capacitance (F), and R_s is the ESR (Ω). From Eq. (8), when $R_s \rightarrow 0$, $\exp(-\Delta V/CvR_s) \rightarrow \exp(-\infty) \rightarrow 0$, and therefore $I = Cv$, meaning the CV curves would be perfectly rectangular (ideal) and, in general, the voltametric curves of supercapacitors display uniquely rectangular profiles in comparison with other electrochemical devices, as can be seen in Figure 6(a).¹³ At this limit, one value for the device capacitance can be determined, called the differential specific capacitance, $C_{d(cv)}$ ($F g^{-1}$), as a function of the scan rate at a specific applied voltage, V^* , which is close to the maximum applied voltage. $C_{d(cv)}$ is given by:

$$C_{d(cv)} = \frac{1}{m} \left(\frac{\partial I}{\partial v} \right)_{V^*}, \quad (\text{Eq. 9})$$

where m (g) is the mass of the active electrode material. In the case where an appreciable ESR is present, a different capacitance value can be determined, called the integral specific capacitance, $C_{int(cv)}$ ($F g^{-1}$), first calculated by integrating the current Eq. (8) with respect to voltage to determine the voltametric charge, q (C), given by:

$$q = \frac{1}{v} \int_{V_0}^V I \cdot dV = C\Delta V - C^2vR_s \left[1 - \exp\left(\frac{-\Delta V}{CvR_s}\right) \right]. \quad (\text{Eq. 10})$$

Here, both the experimental method for determining the charge is given alongside the integral of Eq. (8), demonstrating the theoretical dependence on the ESR. Lastly, the integral specific capacitance can be directly calculated by the definition of capacitance, per unit mass:

$$C_{int(cv)} = \frac{q}{m\Delta V}. \quad (\text{Eq. 11})$$

It is important to note that these equations do not perfectly describe and account for the intricacies of supercapacitor devices. These equations do not allow for the distinction between EDL-capacitance behaviour and faradaic contributions from pseudocapacitance (especially in the limit $I \cong Cv$) and also do not provide consistent capacitance values when applied across a range of scan rates (in the case of differential capacitance) for porous electrodes due to the surface irregularities. However, researchers have devised models to overcome some of these issues, for example, by attributing the variations in differential capacitance values to the presence of internal and external active surfaces only being accessible at certain voltage scan rates due to resistance and mass transport effects.⁶

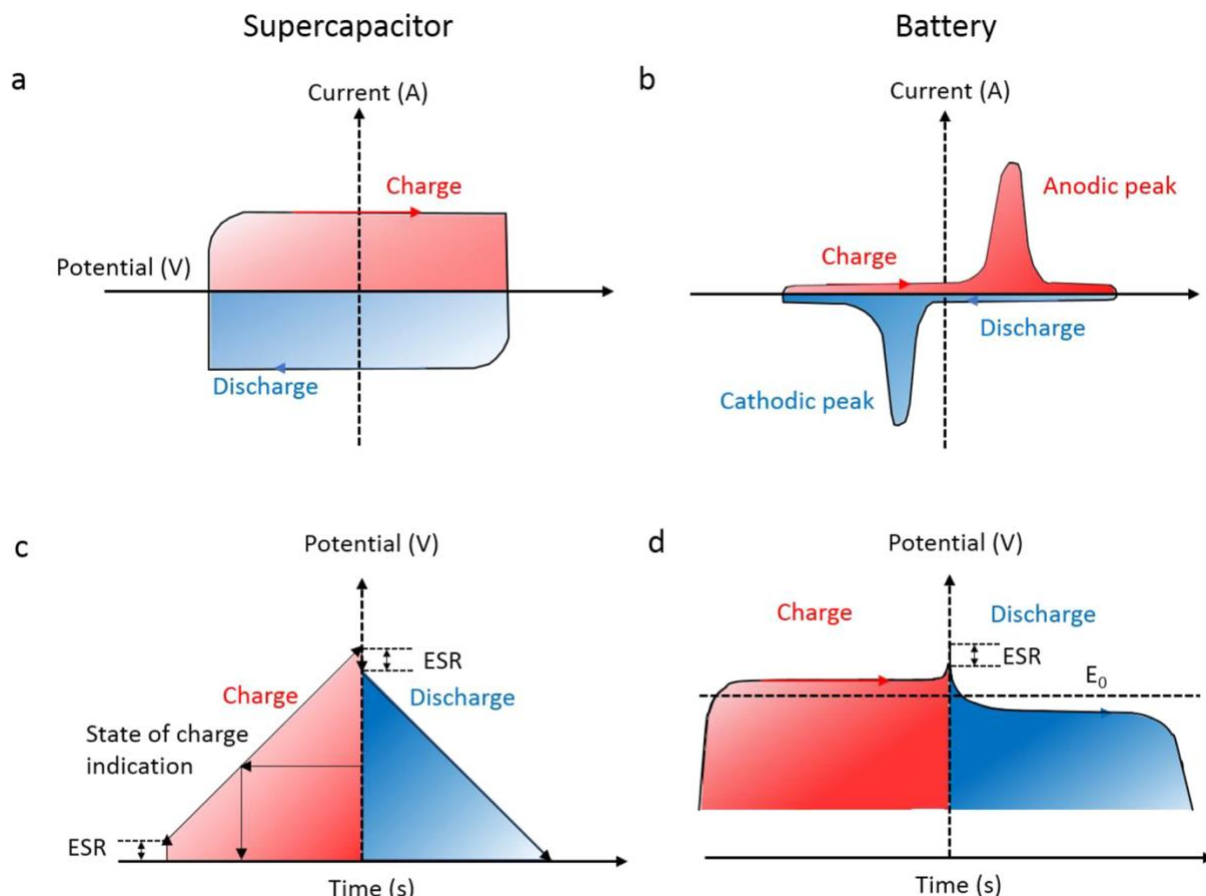


Figure 6: The differences in expected electrochemical response between a typical supercapacitor and a typical battery to cyclic voltammetry (a and b) and galvanostatic charge-discharge measurements (c and d).¹³

5.2.2 - Galvanostatic charge-discharge

GCD measurements involve applying a constant current I across the device in both a positive and negative sense (charging and discharging) over a time t . Therefore, similarly to CV, this measurement allows for many cyclic measurements to be made and is a preferred method for evaluating the cyclability of a supercapacitor device (or any battery technology), with the added benefit of being scalable from the laboratory to the industrial setting, in which this technique is commonly used.¹⁴ However, in contrast with CV which varies voltage at a particular rate, GCD varies time (hence also called chronopotentiometry) while measuring the voltage response V , given by:

$$V(t) = IR + \frac{I}{C}t, \quad (\text{Eq. 12})$$

where R is the resistance and C is the capacitance. For an ideal EDLC, the capacitance is not time dependent, so by Eq. (12) the voltage is linear with time under both current directions, resulting in a symmetrical triangular voltage response, as can be seen in Figure 6(c). The specific capacitance via GCD, $C_{(\text{gcd})}$ (F g^{-1}), can be directly found from the slope of the curve:

$$C_{(\text{gcd})} = \frac{I}{m \left(\frac{\partial V}{\partial t} \right)}, \quad (\text{Eq. 13})$$

where m (g) is again the mass of the active electrode material, and where I and $\partial V/\partial t$ must both be in the same region, either under charging or discharging. The ESR may also be found via GCD and is proportional to the voltage-drop ΔV shown as a discontinuity in the triangular

voltage response upon inversion of the current direction ΔI , as in Figure 6(c). For GCD measurements, a normalising factor of $\frac{1}{2}$ is included,¹⁵ providing the ESR, R_s :

$$R_s = \frac{\Delta V}{2\Delta I}, \quad (\text{Eq. 14})$$

which, along with the capacitance calculations, can be repeated over many cycles to measure the cyclability of the supercapacitor.

However, as with the CV measurements, complications also arise in this technique due to pseudocapacitance and non-ideal EDLC behaviour. For porous electrodes, especially those with a larger concentration of micropores present ($d < 2$ nm) embedded within the larger mesopores, the capacitance is said to be distributed in time, i.e., slower ion penetration for micropores. This distributed capacitance can cause distortions in the voltage response (Eq. (14)) and produce two distinct linear regions, meaning only an average device capacitance can be calculated. The presence of pseudocapacitance can also have this effect, as well as producing a plateau in the voltage response which is characteristic of battery-like behaviour (see Figure 6(d)) and should be discounted from the capacitance calculations.

5.3 – Supercapacitor cell design and applications

The various commercial designs of supercapacitor cells are often specifically tailored for their industrial applications. Besides variations in the basic materials that are necessary for a supercapacitor, such as the electrode materials (the developments of which are discussed later), the electrolyte, and the porous dielectric separator, different supercapacitor cell designs also vary in size, geometry, and orientation of components. Furthermore, the exact details of the manufacturing process such as the order and method of assembly will be intricately linked to the intended application.

Industrial supercapacitor designs can be split in two categories based on size: larger, high-capacitance devices and smaller, low-capacitance devices.¹⁴ The low-capacitance devices are specialised for use in low-cost or small-scale electronics. For example, the first ever commercialised supercapacitor (which was introduced by the Nippon Electric Corporation in 1978 with the brand name “Supercapacitor”) was used to provide backup power for CMOS computer memory in place of conventional batteries. These devices have continued to find use in electronics power management and also as the primary energy-storage system in portable devices, such as children’s toys and power tools.

As a result of the historic use of smaller supercapacitors and the versatility of their application, these devices are highly standardised, taking design inspiration from common electronic components, such as standard electrolytic or dielectric capacitors and coin battery cells. Figure 7 shows the two most-common designs of small-scale supercapacitors, the coin-cell type and wound-cell type.^{6,14,16,17} The coin cell is relatively simple and is therefore commonly used by researchers for prototyping new electrode designs. The relatively long history of the use of these smaller supercapacitors also means that the technology at this scale is already highly optimised and the market is considered ‘quite mature’: any further improvements on existing products are more likely to be in reduced cost and greater robustness than in improved performance (capacitance, energy and power density, etc.).¹⁴

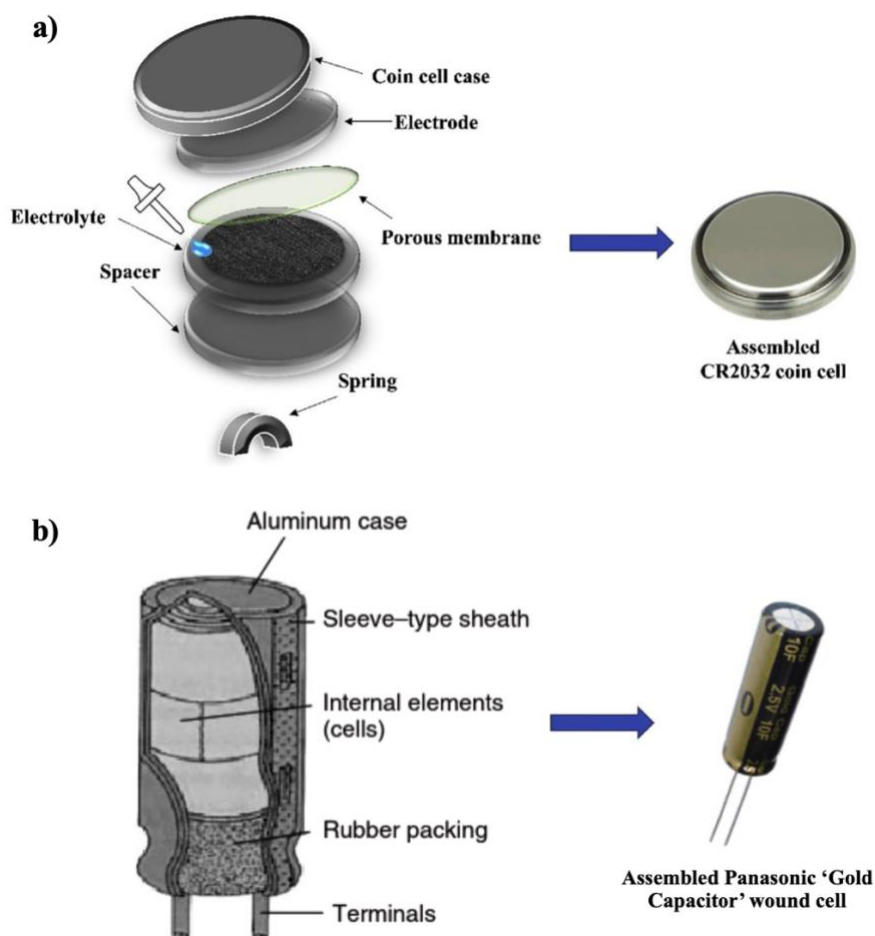


Figure 7: The schematics and assembled images of the two common small-scale supercapacitor design types: a) coin-cell type and b) wound-cell type.^{6,14,16,17}

In contrast, the high-capacitance devices (typically > 350 F) are specialised for heavy-industry applications such as in urban transport, uninterruptible power supplies, automotive hybridisation and heavy machinery. These devices perform in unique circumstances and therefore are rarely standardised and often sold as part of a larger assembly or module, though designs do also take inspiration from other common electrochemical cells. Large supercapacitor designs can be further divided into different types, again based on intended application: high-power cells used commonly in hybrid vehicles and transport, and high-energy cells used commonly in uninterruptible power supplies. Some of the more modern and most expensive designs are both high-power and high-energy cells, for example Maxwell Technologies' (USA) DuraBlue supercapacitors have rated capacitances between 3000 F and 3400 F, with up to 18 kW kg^{-1} specific power and 8.57 W h kg^{-1} specific energy, as shown in Figure 8.¹⁸



Figure 8: Large scale supercapacitor designs by Maxwell technologies (USA). DuraBlue design has capacitance rated above 3000 F, for use in heavy transportation and industry.¹⁸

High-power cells are often very simple in design because this helps to reduce the ESR, which according to Eq. (7), will maximise the deliverable power output of the device. Like with the small-scale devices, the high-power large-scale supercapacitors also employ a spiral wound-cell design as this allows for single pairs of large-surface-area electrodes to be rolled into a single casing. A single electrode pair will have a much lower ESR than many smaller pairs, as is the case with another design type known as a bipolar design, essentially many coin-like cells stacked on top of each other in series. Furthermore, wound cells are much easier to seal than bipolar cells: wound cells only require sealing around the outer can, whereas each individual cell in a bipolar design requires sealing about the electrodes. Bipolar designs are however more efficient in certain circumstances, such as when supercapacitors are connected in series because the additional electrical connections required for wound type cells will add unwanted resistances. Much more emphasis on safety and robustness is given to high-power cells due to their intended use in public transport and hybrid vehicles, meaning these cells are often designed to resist overpressure and be totally sealed (air- and water-tight) to prevent electrolyte leakage.

In high-energy cells, little consideration is given to minimising the ESR, meaning designs can be more complex and allow for much higher energy-density values. One main method to maximise energy density is by using very thick electrodes, which increases the active surface area for EDL capacitance and hence increases energy storage. As before, the advantages of the wound-type cell also apply for high-energy cells and so are often used. In particular, high-energy cells are often modelled after electrolytic capacitors, and many EDLC manufacturers are also electrolytic-capacitor manufacturers, allowing them to use many design ideas in both products, such as using Propylene Carbonate (PC) based electrolytes, employing the same manufacturing processes and using similar casings and electrical connections.¹⁴

Another very important method to increase the energy storage capabilities of large-scale, high-energy supercapacitors is by having one electrode in a cell consist of carbon-based materials (employing EDL-like capacitance) and the other consist of metal ions or oxides (employing faradaic pseudocapacitance). This design is known as an asymmetric or hybrid supercapacitor, being something like half a supercapacitor and half a conventional battery. These devices have shown promising use in all-electric supercapacitor-powered public-transport prototypes.

Supercapacitors have already been very successfully used in hybrid vehicles, both to provide increased power under acceleration and in Kinetic Energy Recovery Systems (KERS, known for its use in Formula 1 racing cars) to recover lost energy under braking and so increase fuel efficiency.¹⁴ However, supercapacitor use in hybrid vehicles is almost always in conjunction with conventional battery technology. In early 2010, Shanghai Aowei

Technology Development Company introduced concepts for fully supercapacitor-powered buses which have since been implemented in city transit routes across the world.¹⁹ Figure 9 shows one of these prototypes implemented in Shanghai, also known as a 'Capabus'. Despite having only about 5% of the energy-storage capabilities of the then best Li-ion batteries, because the supercapacitor cells could be charged so rapidly and repeatedly at bus stops, the low energy-density isn't a problem for suitable routes. These buses used an estimated 40% less electricity compared to electric trolley buses and had lifetime fuel savings of \$200,000 over a diesel bus.²⁰



Figure 9: A fully supercapacitor-powered 'Capabus', premiered at the Shanghai Expo 2010.

5.4 – Supercapacitor electrolytes

Although not the focus of this report, the choice of electrolyte solution for use in supercapacitors is an important factor in their design. The choice of electrolyte solution for a supercapacitor will affect the device's performance, safety and cost, with the main factor influencing these being the voltage and temperature operating windows. Crucially, as per Eq. (6) and Eq. (7) respectively, the energy-storage and power-output capabilities of supercapacitors are both proportional to the square of the voltage window, and the value of the applicable voltage window is dependent upon the electrolyte solution. Typically, electrolyte solutions are split into two categories: aqueous and non-aqueous (or organic).²

Aqueous electrolyte solutions have a low operating voltage of approximately 1 V, because at higher voltages the water molecules begin to decompose, which results in irreversible performance loss.² However, aqueous electrolytes have the advantages of having relatively high electrical conductivity, smaller ion sizes (allowing for increased capacitance in narrow pores), and low cost due to less stringent purification procedures.² Furthermore, aqueous electrolytes are much safer than organic electrolytes as they are less flammable and less toxic, and don't typically corrode or otherwise damage the electrode material. Examples of aqueous electrolyte solutions used in supercapacitors include alkaline metal sulfates (Na_2SO_4 , K_2SO_4 , Li_2SO_4), sulfuric acid (H_2SO_4) and other alkaline metal salts (KOH , LiOH , KCl).²¹

Organic electrolytes have the major advantage of having much higher operating voltages of approximately 2.7 V, which suggests as high as 7-fold increases in power-output and energy-storage over aqueous electrolytes.^{2,22} However, organic electrolytes have significantly lower electrical conductivity, combined with typically larger ion sizes. This results in a reduced specific capacitance, as fewer pore sizes are accessible, and an increased ESR, both of which negatively compensate for the increased performance due to the higher voltage window.²² Furthermore, organic electrolytes have many other disadvantages not present with aqueous electrolytes, such as concerns of high cost, difficulty of purification (no

water content is allowed), and safety, due to the toxicity and flammability of the organic solvents.² Another concern is that common graphitic-carbon electrodes may begin to corrode in organic solvents at high voltages, which presents further safety issues and requires special protective coating and activation procedures.²² Examples of organic electrolyte solutions include lithium-ion salts (LiTFSI, LiPF₆, LiClO₄) and quaternary ammonium salts (TEABF₄) in organic solvents such as acetonitrile (ACN) and propylene carbonate (PC).²¹

Currently, both aqueous and organic electrolytes have widespread use in supercapacitor devices, and their relative pros and cons lend themselves to different applications and markets. Essentially, organic electrolytes display better overall performance, but aqueous electrolytes are safer and cheaper. The choice of electrolyte is also heavily dependent upon the choice of electrode material: the porous electrode structure must match the size of the electrolyte ions, and the surface features such as chemical activation and wettability must be tailored to the electrolyte as well.²²

6 – Developments in carbon-based supercapacitors

6.1 – Activated carbon powders

Activated Carbons (ACs) are the cornerstone of carbon-based supercapacitor electrode design. The original ‘Supercapacitor’, developed by researchers at Standard Oil of Ohio and later marketed by the Nippon Electric Corporation in 1978, was originally made using AC electrodes. Since then, ACs are still the most widely used electrode materials for EDLC designs.^{2,14} Key to their success is their relatively high specific surface area, resulting in increased capacitance and overall performance, and crucially their relatively low cost.

ACs are produced from carbon-rich organic matter, such as wood (also called Activated Charcoal), coal, synthetic polymers and fruit and nut shells, the most popular of which is coconut shell. These carbonaceous materials are then treated using a combination of physical and/or chemical activation methods, the physical activation typically consisting of heat treatment (700-1200 °C) in an inert atmosphere to carbonise the material followed by an oxidation step at high temperature in the presence of CO₂ or steam.² Carbonisation removes unwanted volatile materials within the carbon precursor (such as heteroatoms) and will, depending on the precursor, either promote the formation of aligned ‘graphite-like’ microcrystals, or in the case of ACs made from biomass materials, will form a rigid amorphous structure of disordered graphene layers with irregular penta- or heptagonal defects producing curvature (non-graphitizable carbons).^{14,23} These carbonised products can then be ‘activated’, removing unwanted carbon residues which would otherwise block up the pores, and thereby improving the porosity and increasing the surface area. The physical activation essentially involves burning away these residues and the chemical activation relies on the dehydrating action of particular chemical agents.²³ Chemical activation is usually performed at much lower temperatures (400-700 °C) using phosphoric acid, potassium hydroxide and zinc chloride. The exact conditions for activation will determine the quality of the resulting electrode material. For example the amount of burn off during physical activation, determined by temperature and duration, may both increase surface area and porosity, but also widen the pores and weaken the structure.²³ The end result is a cheap and easy-to-produce carbon electrode material with acceptable electrical and chemical properties, as well as specific surface areas up to 3000 m² g⁻¹.

Despite having a very large specific surface area, ACs also have a wide pore size distribution of macropores (> 50 nm), mesopores (50-2 nm) and micropores (< 2 nm). Figure 10(a) shows a Scanning Electron Microscopy (SEM) image of an AC prepared from coconut shell, with mostly larger macropores resulting from the original cellular structure of the coconut, alongside Figure 10(b) showing an illustration of the typical pore networks found in

ACs.²⁴ As previously discussed, micropores are more often (depending upon the electrolyte size) the largest contributors to the capacitive effect of EDLCs. Although they are necessary to allow for extra micropore formation during the activation process and for effective ion transfer under charging, the mesopores and macropores are much less effective for generating increased capacitance. Therefore, ACs often suffer from having poorly optimised pore-size distributions and hence a relatively low effective specific capacitance, though these can be controlled somewhat by careful selection of precursor material and activation process details.^{23,25}

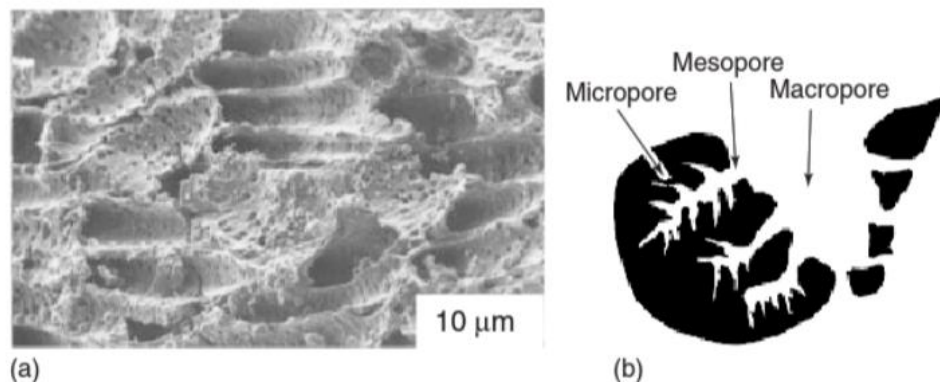


Figure 10: a) SEM image of an AC made from coconut shell, with mostly large macropores (>50 nm) and b) illustration of a typical pore structures found in ACs.²⁴

The effectiveness of ACs for use in supercapacitors is also heavily dependent upon the choice of electrolyte. As per previous discussions, micropore concentration has the most significant effect on capacitance, meaning smaller electrolyte ions, as in the case of aqueous electrolytes, will populate a greater number of micropores than larger organic electrolytes. As a result, aqueous-electrolyte AC designs can reach specific capacitances between 100 and 300 F g⁻¹, whereas organic electrolyte AC designs have typical capacitances below 150 F g⁻¹. Despite this, most commercial AC supercapacitor designs prefer organic electrolytes as they are stable at higher operating voltages up to 2.7 V from below 1 V in the case of aqueous electrolytes.

The surface-functional groups introduced during the activation processes also have a significant effect on AC supercapacitor performance. It has been shown that the presence of carbon surface-functional groups, such as oxygen, can both improve the EDL-like specific capacitance by improving electrode-surface wettability (and therefore improving usable surface area), as well as allow for faradaic pseudocapacitance (a much greater effect).²⁶ This may allow for specific capacitance increases of up to 30 F g⁻¹, with the disadvantage that the functional groups may also catalyse the decomposition of the electrolytes and therefore substantially increase the ESR, leakage current, and tendency for capacitance deterioration over time.²⁷

When making AC electrodes, the AC material (often a powder) is mixed with a conductive carbon material (for example carbon black) and an organic (polymeric) binder before being coated onto the metallic current collectors.¹⁴ This process can be complex, as the interface between the AC film and the current collector can contribute hugely to the ESR of the cell and must therefore be minimised. The nature of the metallic substrate (if it is etched, how clean it is), the nature of the carbon film (the presence of surface functionalities, the carbon morphology and particle size) and the choice of binder are all factors which affect the resulting resistances within the final electrode unit.²³ These factors may be optimised for specific use requirements (power, energy, cost, etc.) by varying manufacturing processes and relative film component (AC, conductive carbon and binder) concentrations.²⁸

In summary, ACs (powders) make very good supercapacitor cells, with reasonable specific surface-area and capacitance values, most importantly at relatively low cost and ease of manufacturing. However, the nature of the activation and manufacturing process means the AC electrodes have a broad pore-size distribution which limits the amount of usable surface area for EDL-like capacitance. This, combined with a typically larger ESR due to poorer electrode-collector connectivity, means powdered-AC electrode designs have limited use.²

6.2 – Activated carbon fibres

Activated Carbon Fibres (ACFs) are another type of carbonaceous material suitable for use in supercapacitors. They are similar to AC powders in that their manufacturing process also involves carbonisation and activation to produce a porous, high-specific-surface-area material which can be optimised for EDL-like capacitance. However, instead of being composed of amorphous graphitic carbon, ACFs are formed from fibrous carbon precursors. Not to be confused with vapour-grown fibres, activated carbon fibres are commonly made from thermosetting organic fibres such as rayon (regenerated cellulose), phenolic resin, polyacrylonite (PAN) and pitch-based materials.^{23,24}

ACFs are formed by first spinning the polymeric precursors, where the molten or dissolved precursor is drawn through a spinneret to produce filament yarns of fibre, before stabilisation, which is essentially a chemical reaction of the fibres with different oxidising gases between 200-400 °C.^{23,24} As with AC powders, these fibres are then carbonised between 800-1500 °C to burn away non-carbon heteroatoms before subsequent activation in an oxidising environment at 400-900 °C. Furthermore, in the same way that the quality of the AC powders depended on the precursor structure and manufacturing parameters, the quality of the ACFs is also dependent upon these factors, in particular, the ordering and alignment of the aromatic constituents of the polymeric precursors. For example, pitch-based ACFs typically have better intrinsic electrical properties than PAN-based ones.²³

The primary advantage of AC fibres over AC powders is that they have a much narrower pore size distribution, predominantly micropores (< 2 nm), allowing for increased EDL-like capacitance. Furthermore, because the fibres have such limited dimensions (typical diameters of approximately 10 µm), the majority of pores are on the outermost surface of the fibres (in contrast with AC powders where micropores are embedded within the large meso- and macropores towards the centre of the particles), resulting in improved active-site accessibility. Ultimately, this results in AC fibres having greater adsorption capacities and adsorption rates, which translates to higher capacitances, lower ESR values and less of a distributed capacitance effect, which finally results in improved specific energy and power values.

Another advantage of AC fibres over powders is the fact that the pore dimensions can be much more easily tuned during the activation process. Therefore, beyond already having predominantly optimal micropore concentrations, these concentrations can also be adjusted to further optimise for specific power or energy storage applications. Figure 11 shows the SEM surface morphology of carbon fibres derived from waste industrial cotton fabrics both after carbonisation (a-c) and then after subsequent KOH chemical activation (d-f).²⁹ The materials retain the precursor cotton's fibrous morphology quite evidently after carbonisation (a-c), but even after activation (d-f) the smaller fragmentations still resemble fibres.

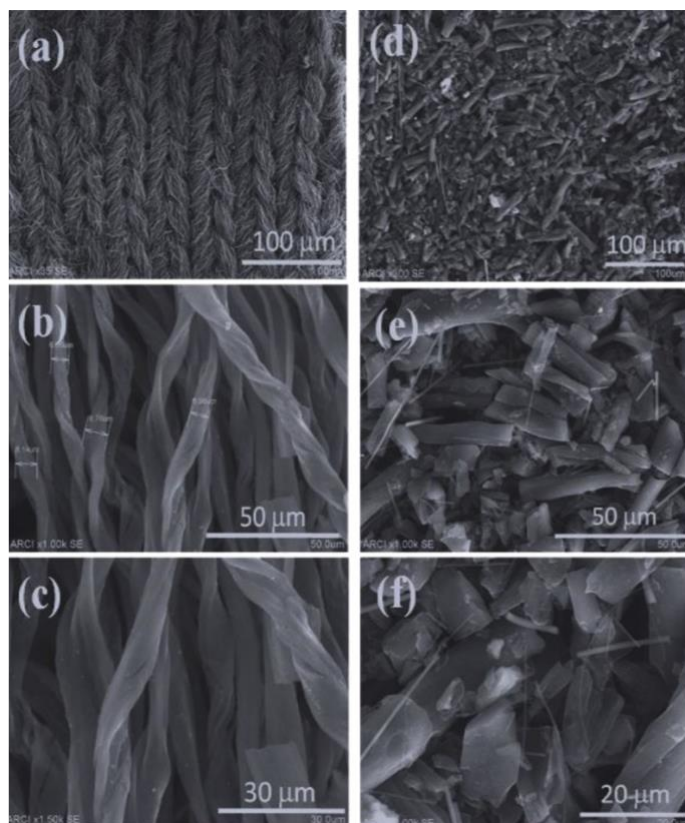


Figure 11: SEM images of cotton-derived carbon fibres: (a-c) after carbonisation, (d-f) after carbonisation and KOH chemical activation.²⁹

The electrodes that were subsequently made from these cotton-derived ACFs were found to have a specific surface area of up to $1550 \text{ m}^2 \text{ g}^{-1}$, while a supercapacitor cell made from these electrodes displayed maximum specific capacitance of 161 F g^{-1} in 6 M KOH aqueous electrolyte and 112 F g^{-1} in 1 M TEABF₄/ACN organic electrolyte. The specific energies of these cells were 6.2 W h kg^{-1} and 29.5 W h kg^{-1} for the aqueous and organic electrolyte, respectively, which compare favourably with other carbon-based supercapacitor electrodes, especially considering that these cells were made from cheap recycled cotton.²⁹ ACF cells made from PAN-based carbon fibres have demonstrated specific surface areas as high as $3291 \text{ m}^2 \text{ g}^{-1}$, with specific capacitance in aqueous KOH electrolyte up to 371 F g^{-1} .³⁰

Though ACFs can also share common problems with AC powders, such as contact resistance at the electrode-current collector interface and performance deterioration due to surface-functional groups, generally AC-fibre cells provide increased surface area, increased electrical conductivity and therefore improved capacitance, power and energy performance over AC powder cells.²³ However, due to the more exotic nature of the carbon-fibre precursors and the additional processing (spinning and stabilisation) required, ACFs cost much more than AC powders, resulting in relatively less usage considering their otherwise favourable properties.^{14,23,31}

6.3 – Carbon Aerogels

Carbon Aerogels (CAGs) are a group of highly porous carbon materials formed by the pyrolysis of organic aerogels which are suitable for use in electrochemical supercapacitors. An aerogel, according to IUPAC definition, is a ‘Gel comprised of a microporous solid in which the dispersed phase is a gas’, where a normal gel is a ‘Non-fluid colloidal or polymer network that is expanded throughout its whole volume by a fluid’.³² CAGs are therefore commonly synthesised by first forming a ‘wet-gel’ via a sol-gel process, where an aqueous

solution of resorcinol (R) and formaldehyde (F) is heated, resulting in polycondensation to form an RF-polymer gel which can be subsequently dried and pyrolyzed (800-1050 °C) to yield a solid matrix of interconnected colloidal-like carbons or polymer chains.³³ The final CAG properties, such as density, pore-size distribution and overall shape and size, can be controlled by varying the sol-gel process and pyrolysis conditions. For example, the density is heavily linked to the ratio of resorcinol and formaldehyde masses to the total mass in solution.^{23,33} As with the AC powders and fibres, the specific surface area of the CAGs can be greatly increased via (physical) activation from as low as 650 m² g⁻¹ to up to 2500 m² g⁻¹, although this results in a relatively small increase in specific capacitance compared with the improvements found under activation of ACs.²³

The resulting CAGs display very good electrical conductivity compared to most ACs and have a very narrow, uniform pore-size distribution consisting primarily of mesopores (2-50 nm) which are very highly ordered and interconnected.^{14,23} Furthermore, CAG electrodes can be manufactured either by mixing carbon aerogel powders with a binder (similar to the manufacturing of AC electrodes) or by creating CAG microspheres, thin films, composites or free-standing monoliths, allowed by the versatility of the sol-gel process.²³ As a result, monolithic CAG electrodes can be prepared without the need for a binder, simplifying the design and minimising the ESR of the supercapacitor cell. The ultralight CAG electrodes can also be made either as flexible polymeric electrodes for use in wound cylindrical cells or as stiff carbon-fibre-reinforced cells in planar coin cells.³³ An example of the latter is shown in Figure 12.³⁴

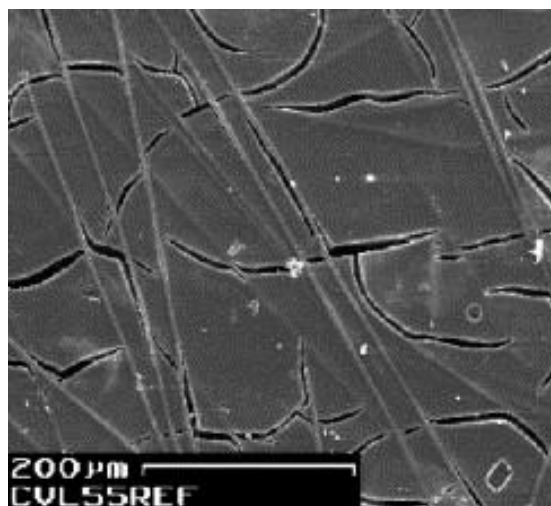


Figure 12: SEM image of a carbon-fibre-reinforced carbon aerogel (pre-activation) with a thickness of 180 μm and a density of 0.544 gcm⁻³. The white-grey stripes are the integrated carbon fibres.³⁴

The combination of a high electrical conductivity, a highly uniform, interconnected mesoporous pore structure (which results in a minimised distributed capacitance) and a lower ESR due to the simplified binder-less electrode designs, results in CAGs having generally high power capabilities.¹⁴ However, specific surface-area values for CAGs are typically in the range of 400-1000 m² g⁻¹ and they are predominantly mesoporous.²³ As before, although activation can drastically increase the specific surface area and introduce microporosity, this results in only a relatively small increase in specific capacitance. As a result, CAGs typically display low specific capacitances, around 80 F g⁻¹ (at 10 mV s⁻¹) even in (higher capacitance) aqueous electrolytes and up to 100 F g⁻¹, meaning poor energy-density values.^{14,35,36}

6.4 - Porous templated carbon

Porous templated carbons are a class of graphitic carbon electrode materials that are also extremely popular for use in supercapacitors, and which are characterised by their

unique method of manufacturing, that is by use of a porous template. As such, there are technically a wide range of electrode-material designs that fall under the category of templated carbons, including nanoporous structures like Carbon Nanotubes (CNTs, which shall be discussed below). But typically what is meant by templated carbons are ‘Microporous’ or ‘Mesoporous’ Carbons: carbon materials with very narrow and well-tailored pore-size distributions that are given by their porous templates.^{2,24}

Generally, templating methods are simple in concept: a chosen porous template structure is first pervaded by a carbon precursor. The system is then carbonised to ‘set’ the carbon network and the template removed leaving just the final porous structure. The method is analogous to baking muffins: one fills the mould with batter, bakes them to set and cook the muffin and then removes the mould before use.² Typically, the templates used for carbon electrode manufacturing are inorganic (often zeolites) and the carbon precursor is an organic polymer. Figure 13 displays an overview of the general templating process used for carbons made using porous zeolite templates.²⁴

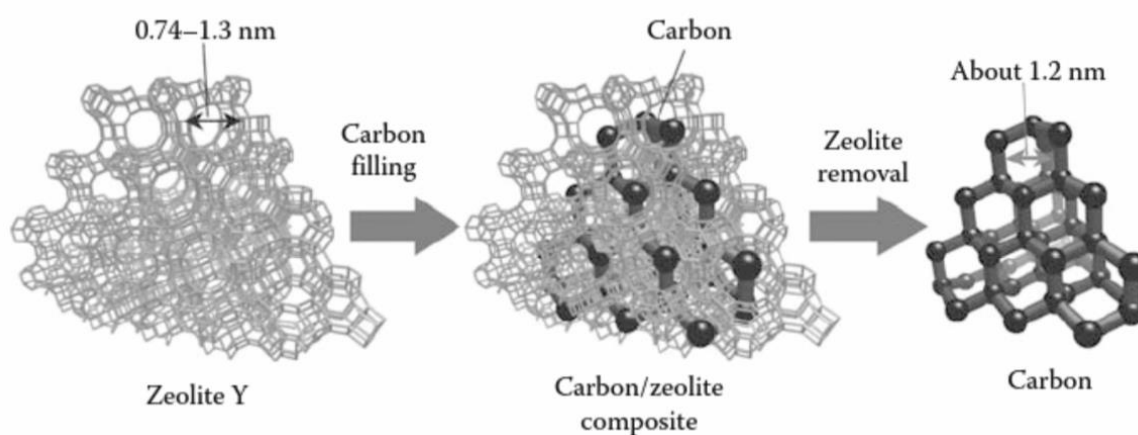


Figure 13: Overview of the carbon templating process using zeolite.²⁴

With reference to the popular work of the group of Kyotani et al.³⁷, a common method is as follows: the inorganic porous template, ‘Zeolite Y’, in the form of a dry powder is mixed with furfuryl alcohol (FA) for 8 hours, before filtration and washing to remove excess FA. The FA impregnated within the zeolite is then polymerised (PFA) by successive heat treatments and under nitrogen flow. To produce the best results, high-temperature propylene gas flow may also be introduced, which results in pyrolytic carbon being further deposited into any remaining openings within the zeolite/PFA composite i.e., a form of Chemical Vapour Deposition (CVD). These two methods can also be used independently of one another to produce the templated carbons.²⁴ Regardless, the zeolite framework is then dissolved by treatment with concentrated HF and HCl acids and the final porous carbon air dried. The materials can also be doped with nitrogen (using acetonitrile in place of propylene) and functionalised with oxygen to increase the hydrophilicity and therefore wettability of the electrode surface by aqueous electrolyte solutions as well as to allow for pseudocapacitance effects.²⁴

The works of the groups of Kyotani et al.³⁸ and Ania et al.³⁹ have focused on producing microporous, N-doped, zeolite-templated carbons via the previously discussed method (PFA impregnation and propylene / acetonitrile CVD) for use in high-energy-density supercapacitor electrodes. These works have produced excellent results, with specific surface areas calculated between 1700-4000 m² g⁻¹, and crucially, an extremely narrow pore-size distribution, with the majority of pores sized between 1.0-1.5 nm and almost no mesoporosity. Figure 14 shows SEM images of a parent Zeolite Y along with 3 types of porous carbons (PFA impregnation + propylene CVD, acetylene CVD, PFA impregnation +

acetonitrile CVD) made by templating onto the parent zeolite, clearly showing the similarity in morphology inherited from the smooth crystalline zeolite surface.³⁸

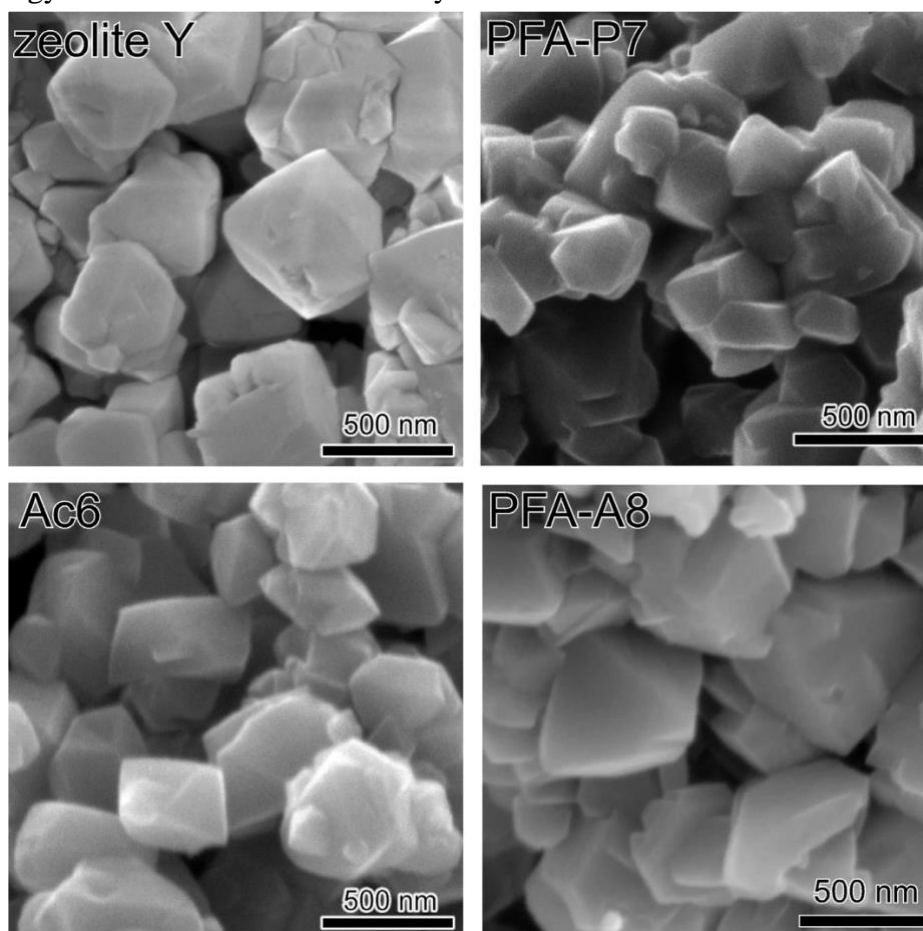


Figure 14: SEM images of parent Zeolite Y and 3 microporous carbons made by templating onto the parent zeolite.³⁸

The specific capacitances of these carbons were found to be very high, with values between 150 F g^{-1} and 350 F g^{-1} (the highest capacitances found using aqueous electrolytes), consistent across a wide range of current densities (up to 200 mA g^{-1}), over a wider-than-typical voltage range (up to 1.2 V) and with good cyclability (of the order of 10^4 cycles). In both studies, the specific capacitance was found to be consistently higher for the N-doped carbons compared to the standard carbons due to the added pseudocapacitance effect allowed for by the nitrogen functionalities. Furthermore, the specific capacitance was shown to deteriorate much less with increasing current density compared with other activated carbon electrodes, such as an AC fibre. This is due to the much more uniform, ordered and interconnected pore networks inherited by these porous carbons from their templates (compared to the much less ordered networks within the standard ACs) allowing for easy electrolyte diffusion, as illustrated in Figure 15.²⁴

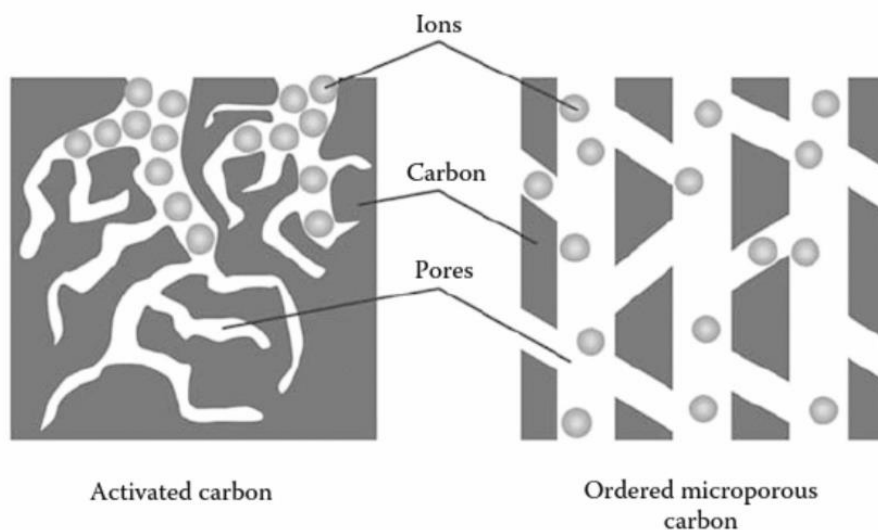


Figure 15: Illustration of the comparison between the complex and less suitable pore network typical of activated carbon electrodes and the interconnected and much more ordered pore network of porous templated carbons.²⁴

The result of the ease of electrolyte diffusion in these microporous templated carbons is that it reduces the distributed capacitance of the supercapacitor devices in which it is used, therefore increasing the specific power and ease of charging and discharging.

This feature can be further tailored by producing templated mesoporous carbons i.e., where a template has been chosen that will result in largely mesoporous electrode films. Mesoporous templated carbons will typically not have as high specific capacitance and energy values as the previously discussed microporous carbons but will have much higher specific power values for high-rate capability supercapacitors. The group of Wang et al. successfully prepared 3D hierarchical porous graphitic carbon (HPGC) electrodes for high-rate supercapacitors. This was a porous structure deliberately ordered to minimise the resistance due to ion transport under charging by having smaller pores successively embedded within larger pores.⁴⁰ Figure 16 shows SEM and TEM images of the different levels of hierarchy in the HPGC material along with a schematic representation of how the hierarchical structure is constructed.⁴⁰

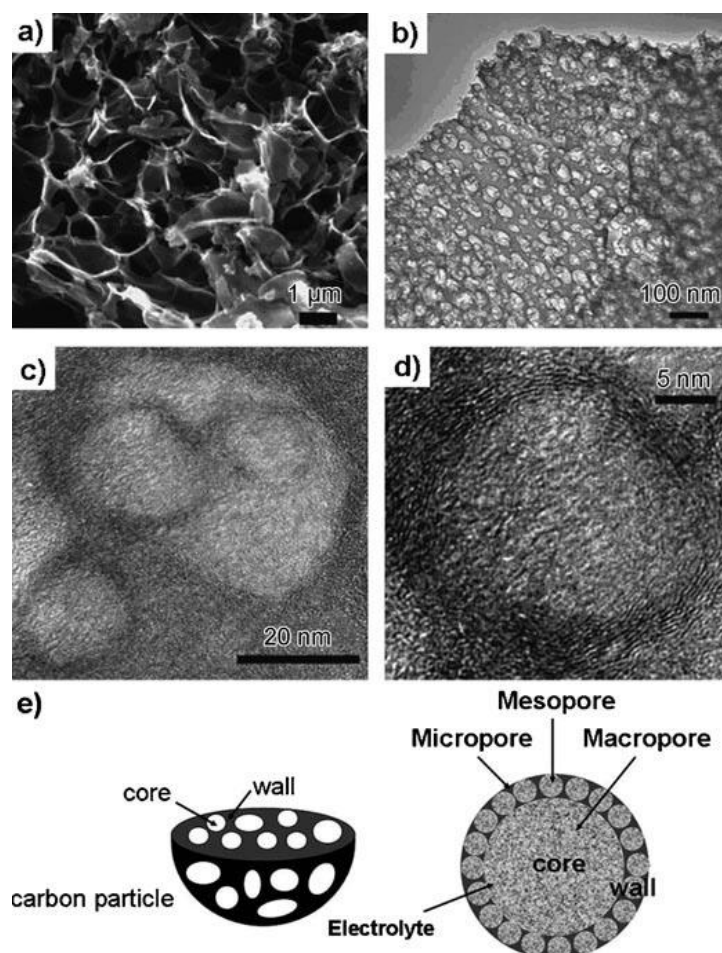


Figure 16: The hierarchical structure of HPGC electrodes. a) SEM image of the microporous cores, b) TEM image of the mesoporous walls, c) TEM image of micropores embedded within the mesopores, d) TEM image of the local graphitic mesoporous walls, and e) illustrations of the overall hierarchical structure.⁴⁰

The largest macropores allow for electrolyte reservoirs to form, with physicochemical properties (such as pathway resistance) similar to that of the bulk solution. The smaller mesoporous walls surrounding these macroporous cores can then act as the most efficient pathway to the large number of micropores within these mesoporous walls. These smallest micropores, as previously mentioned, can then perform their role as the most efficient pore size for EDL-like capacitance to occur. Though the specific surface area of these HPGCs ($970 \text{ m}^2 \text{ g}^{-1}$) doesn't compare so favourably with other AC materials, the fact that the different porous domains can be so carefully ordered to minimise the distributed capacitance and ESR resulted in a promising application for high-power / high-rate supercapacitors, with the HPGC electrodes at the time surpassing power targets for new electric vehicles.⁴⁰

As a result of these advances, the templating method for producing micro- and mesoporous carbon electrodes is viewed as one of the most suitable for producing very-high-performance supercapacitors for use in, for example, hybrid vehicles, as they display the fundamental properties of supercapacitors that are sought after: very high power and rate capabilities, yet with appreciably high energy-storage values as well. There are naturally some disadvantages to the templating method, namely the high expense of the templates used, and the harsh acidic treatments required to remove the templates. Ideally, less expensive templates would be used, such as naturally occurring zeolites and clays, together with less expensive treatment methods e.g., if the template were water-soluble the process would be simpler and cheaper. Another step further would be to use organic, polymer-based

templates, which would require less post-treatment as they would decompose during the carbonisation step, and some groups have recently succeeded in doing this.²⁴

6.5 – Carbon nanotubes

Carbon Nanotubes (CNTs) are one of the more exotic porous carbon materials considered for use as electrodes in supercapacitor devices. CNTs are nanometre-scale carbon structures consisting of shells of single-carbon-wide sp^2 -graphene like layers, formed into long tubes. They are typically split into two categories: individual CNT units known as Single-Walled Carbon Nanotubes (SWCNTs) or nested units of multiple shells known as Multi-Walled Carbon Nanotubes (MWCNTs). Figure 17 shows an SEM image of a SWCNT alongside TEM images of MWCNTs.^{24,41}

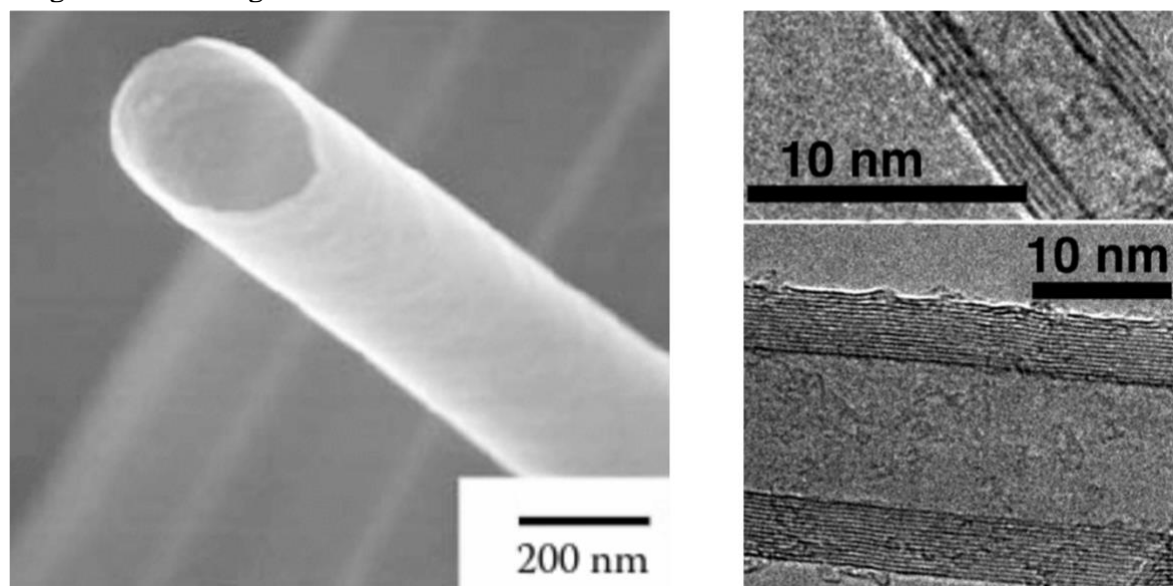


Figure 17: SEM image of a SWCNT (left) and TEM images of MWCNTs (right).^{24,41}

CNTs are manufactured by the catalytic decomposition of various hydrocarbons, the most common and effective technique to do so being CVD. Many methods involve CVD of a hydrocarbon material and a metal catalyst, such as camphor with ferrocene as the gas-phase catalyst, and the iron (from ferrocene) impurities can be subsequently removed by concentrated acid washing.^{4,42} Alternatively, uncapped CNTs with uniform length and diameter can be produced by CVD of propylene into straight nanochannels of an aluminium oxide film, essentially using a form of templating as previously discussed.²⁴ Regardless of method, the synthesis of high purity (i.e., without amorphous carbon and residual catalyst content) CNTs is crucial as they generally have much higher specific surface areas and capacitances, though purity and structure can be controlled by various parameters such as precursor materials, growth temperatures and time.^{23,43}

Fundamentally, CNTs make for good supercapacitor electrode materials as they are naturally porous due to their tube-like morphology, which results in low electrical resistivity and high porosity. The surface area of CNTs is highly accessible, as the pore size distribution is quite narrowly mesoporous, coming from spaces between entangled CNT units, with the minimal concentration of micropores coming from accessible internal nanotube surfaces. These properties make CNTs ideal for use in high-power applications, as the low electrical resistivity and high electrolyte accessibility due to mesoporosity result in a lower ESR and minimised distributed capacitance, which result in high-power capabilities. However, CNTs suffer from having markedly low specific surface areas, with typical CNTs (i.e., with no other structural features or functionalisation) having surface areas less than $500 \text{ m}^2 \text{ g}^{-1}$. This,

combined with their comparatively low micropore concentration, results in CNTs having unimpressive specific capacitance values in the range of 20 to 80 F g⁻¹.

Efforts to further improve the active specific surface area and capacitance of CNTs include surface functionalisation via chemical activation, design of polymer-CNT composite materials, and direct growth of dense, vertically aligned CNT forests onto current collector substrates. In 1996, the group of Niu et al. developed catalytically grown MWCNTs for supercapacitor electrodes and compared untreated MWCNTs with chemically activated MWCNTs, where oxygen surface functional groups were introduced onto the carbon surface by etching with nitric acid.⁴⁴ The as-produced CNTs had an average diameter of 8 nm, but the average pore diameter of the activated electrodes was 9.2 nm, confirming that the large mesoporosity of CNTs is from the inter-tubular pores of the entangled network. The chemical activation was found to increase the specific surface area of the material from 250 m² g⁻¹ to 430 m² g⁻¹, contributing to an improved 102 F g⁻¹ specific capacitance (over previous CNT electrodes) using sulfuric acid electrolyte and an estimated specific power of over 8 kW kg⁻¹. However, at the time, micropores were still considered to be inaccessible to electrolyte ions for EDL-capacitance and were not considered.

In 2002, the group of Frackowiak and Beguin et al. prepared MWCNTs for supercapacitor electrodes that had been further chemically activated using potassium hydroxide (as used for ACs) to increase the surface area and introduce some microporosity.⁴⁵ The activation was found to increase the specific surface area by an average of 635 m² g⁻¹, in one case from around 430 m² g⁻¹ to above 1000 m² g⁻¹. This was due to the activation inducing defects in the CNT walls: increasing the total surface area by the significant inclusion of microporosity, while retaining high mesoporosity by minimally affecting the previous nanotube morphology. As a result, the specific capacitance was shown to increase from a low 15 F g⁻¹ up to 90 F g⁻¹ in aqueous electrolyte (65 F g⁻¹ in organic electrolyte) after KOH activation.

Increasing microporosity in CNTs has also been achieved by preparation of polymer-CNT composites. The group of An et al. prepared SWCNTs by arc discharge and mixed them with poly(vinylidene dichloride) (PVDC) which acted both as a binder to prepare the electrode and helped to create microporosity after the SWNT-PVDC mixture was heat treated.⁴⁶ For the samples treated at 1000°C, the specific surface area was a relatively low 357 m² g⁻¹, but the concentration of micropores reached a maximum, resulting in a high specific capacitance of 180 F g⁻¹. The specific power and energy were found to be 20 kW kg⁻¹ and 6.5 W h kg⁻¹, respectively. An et al. also produced another-high capacitance supercapacitor electrode using a polymer-CNT nanocomposite, where the polymer was uniformly coated onto the nanotube surface and allowed for faradaic pseudocapacitance. The SWCNTs were again produced by arc discharge and placed in solution with polymerisation oxidants before dropwise addition of the polymer, polypyrrole (Ppy), resulted in uniform coating of the nanotube surfaces. Figure 18 shows SEM images of the as-grown SWCNTs, pure Ppy and the SWCNT-PPy nanocomposite.⁴⁶

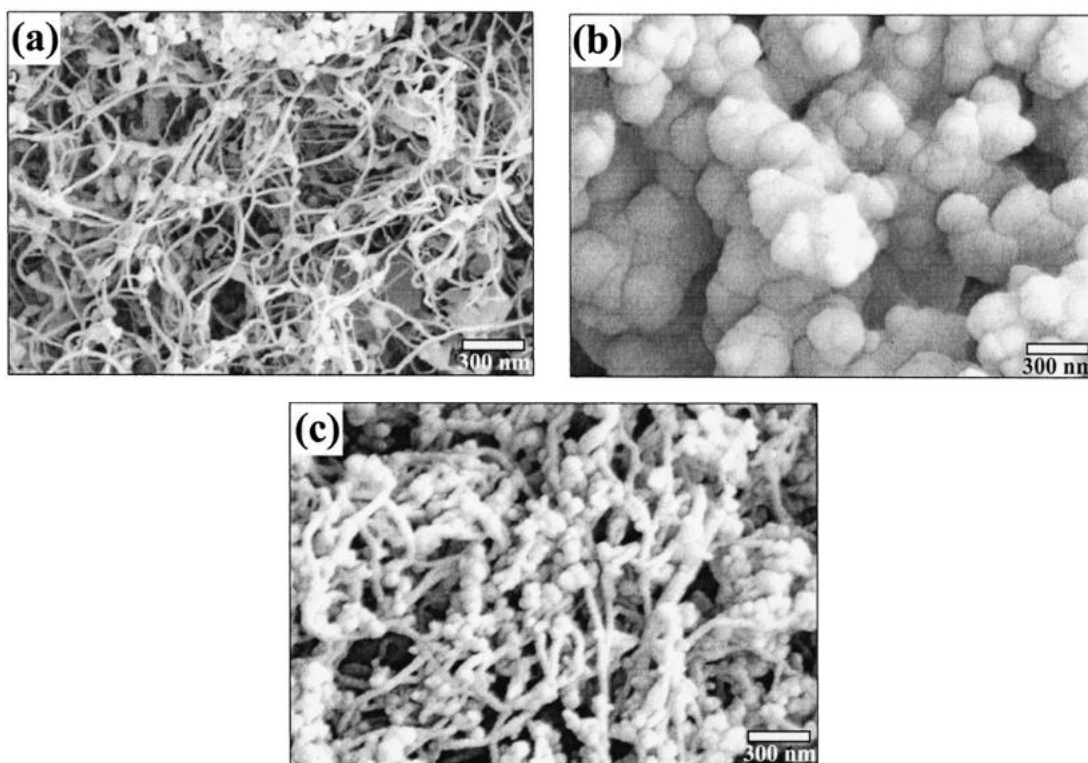


Figure 18: SEM images of (a) as-grown SWNTs, (b) pure Ppy and (c) SWNT-PPy nanocomposite.⁴⁶

Although the specific surface area of the SWCNT-Ppy nanocomposite was only $65 \text{ m}^2 \text{ g}^{-1}$, the effect of both EDL-like and faradaic-like capacitance resulted in a remarkable increase of specific capacitance up to 265 F g^{-1} when also combined with an acetylene black conducting agent which also reduced the ESR of the supercapacitor cell.

Lastly, improvements in CNT supercapacitors have been sought by maximising the efficiency of electrode formation. CNT particles are still commonly bound to the current collector by tedious fabrication methods, often involving binder materials, and this results in unnecessarily high contact resistance.²⁴ Alternatively, what are known as Vertically Aligned CNT (VACNT) forests can be directly deposited onto a current collector to both simplify device fabrication and minimise contact resistance. In 2001, Chen et al. prepared CNT electrodes by direct, nickel-catalyst-seeded CVD growth onto graphite foil which produced a high specific capacitance of 115.7 F g^{-1} at a high scan rate of 110 mV s^{-1} in aqueous electrolyte.⁴⁷ In 2006, Futaba et al. demonstrated the ability to develop highly ordered VACNT forests by CVD which could be subsequently collapsed by a process of wetting and drying that caused the aligned CNTs to ‘zip together’ via capillary forces.⁴⁸ This resulted in an approximate 20-fold increase in the material density, as demonstrated by the diagrams in Figure 19.⁴⁸

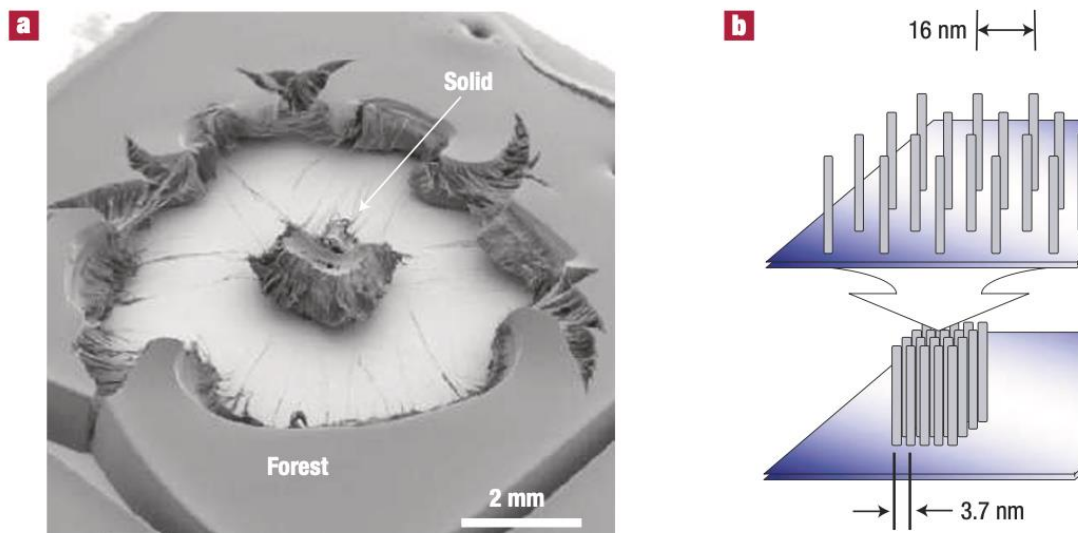


Figure 19: Displays of the higher density of VACNT forests after wetting-drying collapse: a) showing an SEM image of the VACNT forest collapse from a single droplet and b) showing the schematic representation of this collapse.⁴⁸

This process allowed for the scaling up of CNT electrodes without comprising the nanoscale properties of the individual CNT units, such as high surface area and electrical conductivity, and resulted in a specific capacitance of 80 F g^{-1} , and an energy density of 69.4 W h kg^{-1} .

Despite continued improvement of the specific energy storage of supercapacitors manufactured from CNTs, these results are still typically lower than what can be achieved with other high-surface-area carbons, which are also often much cheaper than CNTs.²³ As a result, CNT-electrode usage in supercapacitors is normally restricted to high-rate applications (specific powers above 8 kW kg^{-1}) and have promising use for microelectronics applications.¹⁴

6.6 – Summary of graphitic carbon supercapacitor electrodes

Aside from the inclusion of metal oxides and other pseudocapacitance-inducing materials, the history of supercapacitor electrode design has been predominantly the development of graphitic carbon materials. Those include materials previously discussed, such as activated carbons, activated carbon fibres, carbon aerogels, porous templated carbons and carbon nanotubes, as well as many others that haven't been included in this review such as graphene⁴⁹, glassy carbons²³ and carbide-derived carbons²⁴. All of these materials are based on generally amorphous sp^2 -bonded graphene-like carbons ranging from the highly disordered activated carbons to the more ordered forms of templated carbons and carbon nanotubes. They are all materials with uniquely advantageous surface areas, pore-size distributions and surface functionalities that are appropriate for varying applications, but the materials (such as porous templated carbons) for which these properties can be very finely tuned have an associated cost that compares poorly with the extremely cheap activated carbons. Regardless, the search for high-performance supercapacitor-electrode materials continues, and one approach that has begun to be taken in recent years is to switch from sp^2 -bonded graphitic carbons to sp^3 -bonded diamond.

7 – Diamond-based supercapacitors

7.1 – Suitability of diamond for supercapacitor use

Apart from their obvious and historic association with wealth and jewellery, diamond has long been a fascinating material due to its unique and extreme material properties. Diamond is commonly known for being the hardest naturally occurring material but is also the material with the highest thermal conductivity (lowest coefficient of thermal expansion) and boasts many other favourable properties.⁵⁰ Diamond is also chemically inert, is resistant to wear and is broadly optically transparent. Unfortunately, naturally occurring diamond is also an extremely good electrical insulator, being a very-wide-band-gap semiconductor, and so has electrical resistivity of the order of $10^{16} \Omega \text{ cm}$.⁵¹ Fortunately, diamond can be doped with boron to introduce charge carriers, giving it a p-type semiconducting character. This material is known as Boron-Doped Diamond (BDD), and, depending on the doping level, BDD can have electrical conductivity values approaching that of metals. Any reference to diamond-based supercapacitors or electrodes is necessarily a reference to electrically conducting BDD. BDD retains the other chemical and physical properties of naturally occurring diamond, and so is an extremely durable and chemically inert material that can be used for electrodes. Figure 20 shows SEM images of both undoped and boron-doped diamond.⁵²

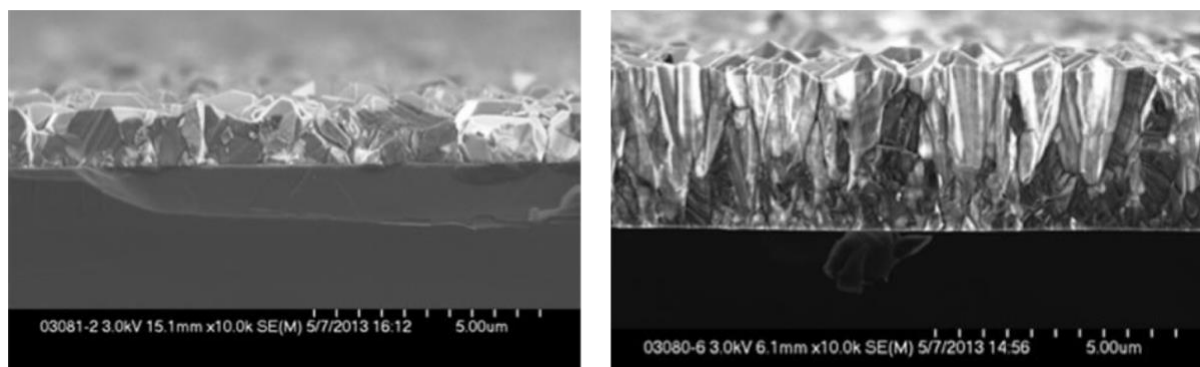


Figure 20: SEM images of undoped diamond (left) and BDD polycrystalline films grown by CVD (right).⁵²

The primary advantage BDD electrodes have over graphitic carbon electrodes relates to their chemical inertness, that is, diamond can be used over a much wider range of voltages than graphitic carbon, both using aqueous and organic electrolytes.⁵¹ With graphitic carbons, applied voltages above approximately +1 V result in the decomposition of the water within aqueous electrolyte solutions. Non-aqueous electrolytes with voltage ranges above 2.7 V cannot be used as they corrode the graphitic carbon electrode. However, diamond electrodes lack the required catalytic binding sites that are needed for the initiation of electrolyte decomposition in aqueous solutions, allowing voltage ranges between 3 and 3.5 V.⁵¹ Furthermore, diamond doesn't corrode in many of the harsh organic solutions that corrode graphitic carbon, such as concentrated nitric (HNO_3) and sulfuric (H_2SO_4) acid, allowing for voltages as high as 7.5 V.^{51,53} BDD electrodes have been used over a voltage range of -35 to +6 V in 2 M H_2SO_4 without damage.⁵³

First, this extreme chemical stability would allow for effective use of BDD electrodes for long-lifetime applications, for example in devices that are difficult to repair or require constant use (such as in critical power-supply applications). However, much more important an advantage is that the overall increase in applicable voltage corresponds to a massive step up in performance, because both the storable energy and applicable power of a supercapacitor are proportional to the square of the applied voltage (Eq. (6) and Eq. (7), respectively).

Therefore, the improved voltage range of diamond electrodes indicates a possibly significant improvement in performance over previous graphitic carbon designs.

7.2 – Reports of diamond supercapacitors

The earliest reports of BDD electrodes with a view towards applications in supercapacitors were published around the year 2000 by the group of Masuda et al., in which they prepared nanostructured diamond honeycomb films by a top-down plasma etching approach.⁵⁴ In this work, nanostructured Anodic Aluminium Oxide (AAO), a material also used as a template for CVD growth of CNTs, was used. However, in this work the AAO was used as a mask instead of a template, placed above an unstructured diamond film to create a honeycomb network after oxygen plasma etching. Figure 21 shows a schematic diagram of the procedure for generating the nanoporous diamond honeycomb alongside an SEM image of the prepared honeycombs.⁵⁴

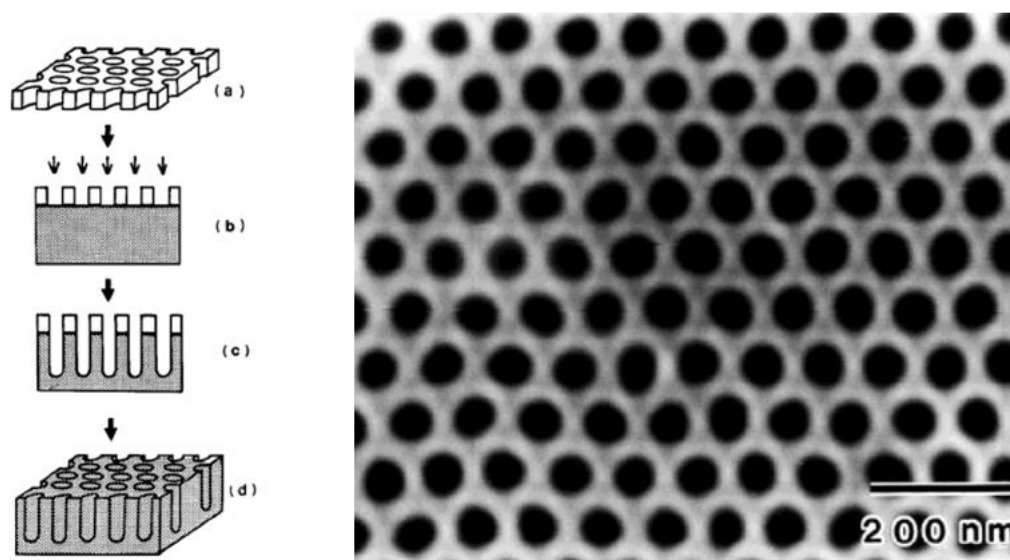


Figure 21: Left: schematic diagram of the fabrication process for diamond nano-honeycombs. a) honeycomb AAO mask, b) placement of AAO mask on diamond film with subsequent oxygen plasma etching, c) the resulting etched diamond film with the mask and d) with the mask removed. Right: SEM images of the diamond nano-honeycomb.⁵⁴

Though these diamond films could be used over a much wider voltage range (approximately 7.3 V in organic and 3.5 V in aqueous electrolytes), the specific capacitance and surface areas of these films were relatively low.⁵⁵ For the purposes of comparison, early BDD nanostructures had specific (area) capacitances of the order of $150 \mu\text{F cm}^{-2}$ and surface areas of the order between 30 and $60 \text{ m}^2 \text{ g}^{-1}$.⁵³ Activated carbon electrodes are known to have specific capacitances of the order of 1 F cm^{-2} and surface areas of between 2000 and $3000 \text{ m}^2 \text{ g}^{-1}$. As a result of the poor specific areas and capacitances achieved by these nano-diamond supercapacitors, development of higher porosity and surface-enlarged diamonds was required.⁵³

Reports of the development of porous templated BDD supercapacitor electrodes only began to be published around the year 2015. Gao and Nebel published an article at this time, both reviewing efforts to prepare diamond supercapacitor electrodes using a templating method and presenting a novel method of their own, with which they prepared what they considered to be “the first prototype pouch-cell device based on free-standing diamond paper” (with only two electrodes).⁵³ The methods their group developed take inspiration from the porous templating method used to manufacture meso- and micro-porous graphitic carbon electrodes as previously discussed, attempting to achieve the same large surface areas and

easily adjustable morphologies with diamond. Earlier templating methods demonstrated include the use of nanodiamond-seeded silicon nanowires grown over with diamond by microwave plasma-enhanced CVD (MWCVD) and cheaper and easy to remove SiO₂ foams also grown over by CVD.⁵³ Though these methods resulted in surface area increases over planar diamond electrodes of between 40- and 150-fold, templated-diamond growth via CVD is much more difficult than sp²-graphitic templated growth. This is because the previously discussed graphitic templating methods involve a liquid-phase precursor that is carbonised and supplemented by CVD growth, meaning the liquid precursor can be easily mixed with the template and uniformly coat the template surface. In comparison, CVD diamond growth relies solely on the ability of reactive gaseous radicals to diffuse through the complex 3D structure. Therefore, the tendency is for the reactive species to decrease in kinetic energy as they penetrate the internal structure and be less likely to react to form diamond, resulting in well-deposited diamond at the template surface with more non-diamond carbons deposited further into the core of the template. The comparison between the ease of templating in graphitic carbons and diamond carbons is demonstrated in Figure 22.⁵³

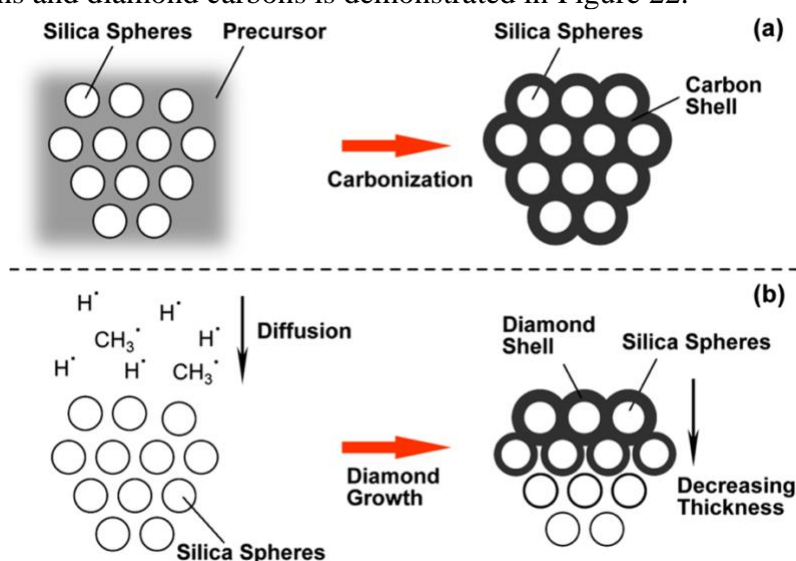


Figure 22: Schematic comparison between the porous templated growth of (a) sp²-graphitic carbon using a liquid precursor and (b) diamond using gaseous precursors.⁵³

The group of Gao et al. developed a method of layer-by-layer growth, where a monolayer of SiO₂ spheres were spin-coated on a BDD surface, seeded with nanodiamond and covered with diamond by CVD, with as many of these layers as desired being subsequently built on top of one another with uniform diamond deposition before the template is removed. Unfortunately, this layer-by-layer process was deemed to be far too laborious and time consuming for realistic industrial applications. Ultimately, Gao and Nebel settled on a porous template made of high-quality quartz filters (based a glass-fibre filter template method but allowed for high temperature CVD) that had a larger average pore size than the SiO₂ foams (2.2 μm over 0.5 μm) and so allowed for deeper diamond penetration. The as-deposited films were subsequently cleaned of extra sp²-carbon using boiling H₂SO₄ and HNO₃ and then the underlying silicon substrate was removed to produce a free-standing porous diamond paper. Figure 23 shows SEM images of the final porous diamond paper, with zoomed-in images across the depth of the paper showing the still significant effect of diffusion limitation of the gaseous reactants.⁵³

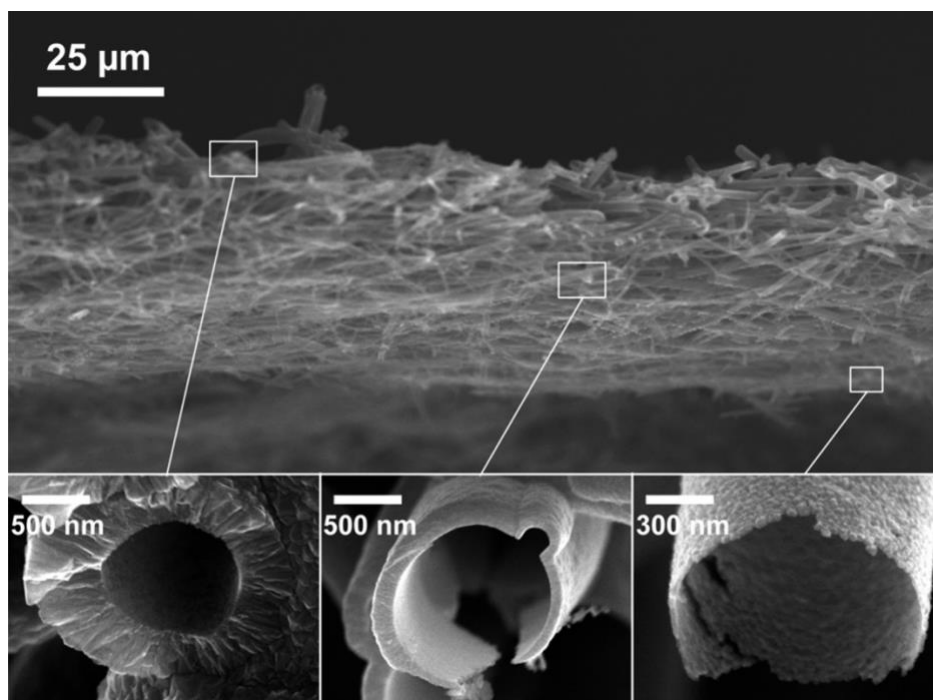


Figure 23: SEM images of the freestanding porous diamond paper, with zoomed-in images across the depth of the paper showing decreased layer thickness due to diffusion limitation.⁵³

A prototype 2-electrode supercapacitor device was then constructed using stainless-steel current collectors and 3 M NaClO₄ aqueous electrolyte solution. As expected, the cell was able to be used across a voltage range wider than usual for aqueous electrolytes due to the non-catalytic diamond surface, with perfectly rectangular CV profiles below 1.2 V and cycle efficiency above 80% even at very high voltages up to 2.5 V. This ‘low’ value of 2.5 V is a result of remaining sp²-carbon content even after cleaning, and the authors suggest with better cleaning of the diamond electrode, voltages as high as 3.5 V could be possible. However, although the specific capacitance of this device was shown to be an improvement over the previously prepared SiO₂-templated diamond foam, the value was less than 0.7 F g⁻¹ which is 2-3 orders of magnitude lower than sp² carbons. This was deemed to be due to the unnecessarily thick (0.5 μm at the topmost layers, see Figure 23) diamond coatings causing material inefficiency. The resulting trade-off between-high voltage window and low specific capacitance meant a high specific power of 100 kW kg⁻¹ but a low specific energy of less than 1 W h kg⁻¹.

In 2016, the group of Moreira et al. also developed a porous-templated supercapacitor electrode material by a method of BDD growth onto vertically aligned MWCNTs (VACNTs).⁵⁶ This technique has the advantage of achieving both the high surface area and controllable porosity of CNTs with the desirable chemical properties including the wide voltage window of diamond. First, VACNT films were prepared by microwave plasma CVD onto either Si or Ti substrates seeded with Ni nanoparticles to help promote the subsequent CNT growth (using CH₄ gas). The VACNTs were further activated by plasma-enhanced CVD to introduce oxygen functionalities and improve wettability. The as-prepared VACNT forests were then electrospray-seeded with nanodiamond to produce honeycomb-like microstructures with the individual CNT tips joined together. BDD CVD growth was subsequently performed (in CH₄/H₄ with diborane, B₂H₆) to deposit a 0.25-0.5 μm layer of BDD crystals. It is worth noting that the layer thickness produced here is of the same order of the layer thickness of the middle-to-outermost sections of porous diamond paper prepared by Gao and Nebel.⁵³ The honeycomb ‘crests’ consisted of between 10 and 1000 individual CNTs connected side-by-side with an areal tube density of the order of 10⁷ cm⁻², much less

than the 10^{12} cm^{-2} prepared by Futaba et al. when they prepared high-density collapsed VACNT forests.⁴⁸ Figure 24 shows SEM images of the VACNT-BDD electrodes prepared on a Ti substrate (referred to as Ti/VACNT/BDD) with varying levels of magnification and showing the honeycomb-like ridges that form the electrode microstructure.⁵⁶

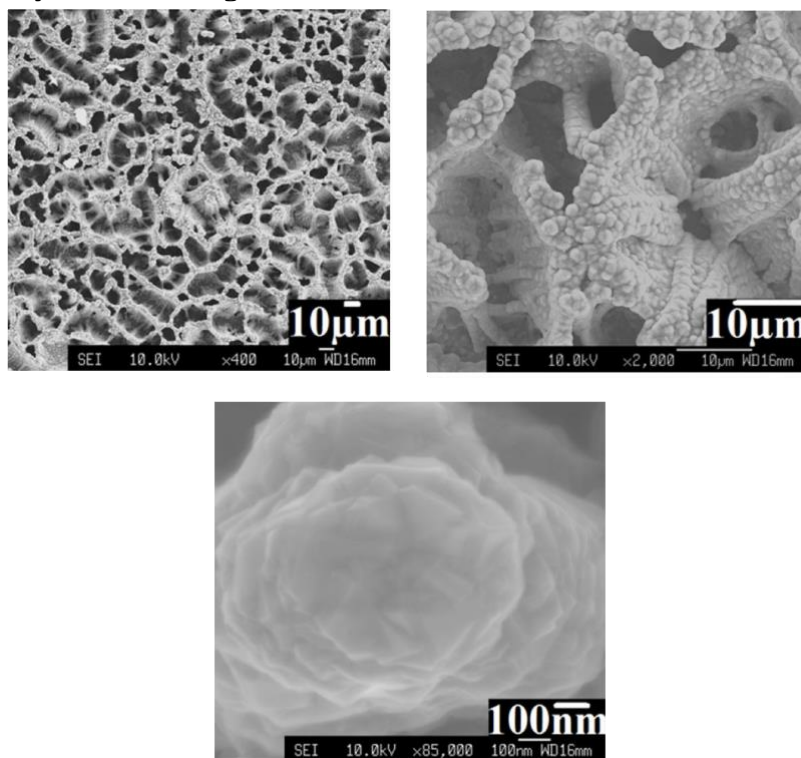


Figure 24: SEM images of Ti/VACNT/BDD with varying levels of magnification.⁵⁶

The supercapacitor cell design used was a custom-built polyacrylate housing with stainless-steel current collectors, designed to be easy to handle and exchange materials contained. The electrolyte solution used was a solid / gel-like paste made of dilute PVA and concentrated phosphoric acid which could be spread across the electrode surface. The best results for the various electrodes prepared were from the Ti/VACNT/BDD sample grown for half an hour and so only these are mentioned here. The electrochemical results of this device are somewhat mixed: the specific capacitance, both gravimetric and areal, showed improvement over the porous diamond paper prepared by Gao and Nebel, with values of around 8 F g^{-1} and 1 mF cm^{-2} over 0.7 F g^{-1} and 0.6 mF cm^{-2} , respectively. The specific energy was also of the order of less than 1 W h kg^{-1} , but the specific power was only 176 W kg^{-1} in this paper compared to 10^5 W kg^{-1} achieved by porous diamond paper, though this is in part due to the limited voltage range of 1 V used in the CV and GCD measurements.

One of the most recent developments in diamond supercapacitors was published in 2019 by the group of Wang et al., in which they prepared a 3D porous BDD film by CVD growth onto a porous titanium template / substrate.⁵⁷ Here, BDD was directly grown onto pre-washed and treated porous Ti films by hot filament CVD, and Figure 25 below shows the SEM images taken of the substrate before and after BDD deposition.⁵⁷

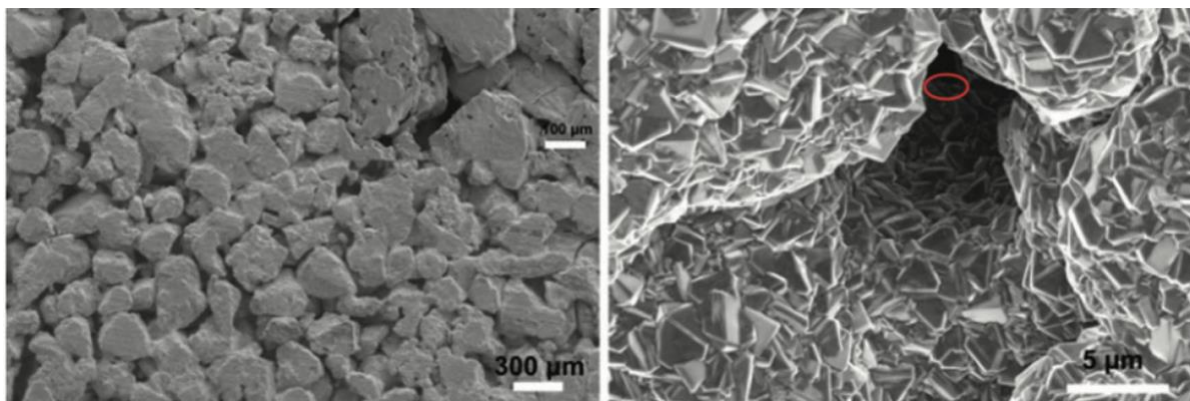


Figure 25: SEM images of the 3D porous titanium substrates before (left) and after (right) deposition of BDD films.⁵⁷

As is indicated by Figure 25, the average pore size of the material is still very high, with an average of 32 μm , but the cell prepared displayed a much-improved specific capacitance over previous diamond electrodes, with a value of 6.02 mF cm^{-2} . This combined with the expected wide voltage window (2 V) as well as high-rate capability and cycle durability resulted in good specific power values and relatively high specific energy values for BDD supercapacitors.

7.3 – Summary of diamond supercapacitor electrodes

In summary, diamond-based supercapacitor devices have been reported in literature, with the most promising results coming from electrodes manufactured by BDD CVD growth onto porous templates. These devices make good use of the chemical properties of diamond, allowing for wider voltage ranges to be used, but can also be made to have higher surface areas than planar diamond electrodes, increasing specific capacitance, energy and power. The wide voltage range and porosity allow for very high specific-power values to be achieved and so suggest diamond supercapacitors could be used for high-rate applications. However, due to the difficulties associated with CVD on porous templates and the typically large grain size of deposited diamond, the average pore sizes within diamond supercapacitors are of the order of micrometres instead of nanometres, meaning negligible micro- and meso-porosity and relatively low specific area when compared to conventional graphitic carbons. Therefore, the specific capacitance and energy of diamond supercapacitors do not yet compare favourably with conventional supercapacitors and are therefore limited to high-rate applications, unless methods of introducing significantly lower pore sizes can be introduced.

Another approach involves the introduction of pseudocapacitance to BDD electrodes by the addition of metal oxides. Though this has been shown to increase the specific capacitance to around 350 F g^{-1} which is comparable with graphitic carbon electrodes, the relatively weak adhesion between the BDD and metal oxides results in comparatively poor cyclability.⁵⁸ Instead focussing on the unique high-rate power applications of these devices, diamond supercapacitors can continue to be improved by further widening the voltage window: an increase of voltage from 2.5 to 3.5 V for aqueous solutions could result in a 100% increase in power and energy.⁵³ The specific capacitance may also be increased (though likely not to the level of graphitic carbons) by further improvements to templating and etching methods in order to increase the density of the holes or pores and reduce their size.⁵³ Estimations made of the possible performance of porous diamond supercapacitors place the potential specific power as high as 4 MW kg^{-1} and specific energy as high as 12 W h kg^{-1} .⁵³ Therefore, diamond is still a promising material for improved supercapacitor performance.

8 – Conclusions

In conclusion, the fundamental concept of a supercapacitor, their theorised mechanisms of operation, their applications and their historical developments have been discussed. Supercapacitors are a form of charge-storage device that operate by the close separation of a porous electrode and electrolyte charges which induces a capacitance. This, combined with a possible added effect of battery-like pseudocapacitance, allows for energy to be stored and released at uniquely high rates (or power) in the case of supercapacitors. The high-rate and appreciably high energy-storage capabilities of these devices allow for them to be used in a wide variety of industrial applications, from small scale electronics to heavy machinery, with the hope of further developments of these devices enabling a new generation of super-fast charging electric vehicles.

Many factors contribute to the success of supercapacitor electrode materials, but key among these are very high surface areas, unique pore-size distributions (particularly high micro- and meso-porosity), low device resistance, wide applied-potential range and always of importance in industry, cost. The material which has so far best met these criteria and been widely used for supercapacitor electrodes is graphitic-sp² carbon. These materials are often made from very cheap carbon precursors, can be activated to massively increase their specific surface area, wettability and porosity, and the exact different forms of graphitic carbon can be tailored for differing applications, such as microporous carbons for high energy storage and mesoporous carbons for high power output.

An alternative form of carbon, namely (boron-doped) diamond, has also been proposed as an excellent material for supercapacitor devices and in recent years such devices have been prototyped with varying success. Crucially, the chemical inertness of diamond allows for much higher voltage ranges to be applied, and as both the power and energy storage have a squared dependence on voltage, this results in ideally large increases in performance over graphitic carbon devices. However, porous diamond is much more expensive and difficult to make because the common method of chemical vapour deposition results in non-uniform layer growth and essentially prevents micro- and meso-porosity in diamond electrodes. As a result, diamond supercapacitors are incomparable with graphitic carbons when it comes to specific area, capacitance and energy storage, but do show promising results for use in specialised high power / high-rate applications which might otherwise rely on conventional capacitors or electrolytic capacitors (which have very low energy storage).

Though the exciting possibility of fast-charging electric vehicles may not be realisable with diamond supercapacitors, they are still a promising charge-storage device with their own unique applications and advantages. Further development of diamond supercapacitors will likely focus on: continued efforts to increase the applicable voltage by use of suitable electrolyte solutions and increased diamond purity; the inclusion of pseudocapacitance-inducing active species on the electrode surface to further increase overall performance while avoiding issues of cyclability (though pseudocapacitance has only minimally been discussed in this report); further improvements of CVD templating or etching methods to further increase the specific surface area and aim to reduce the average pore diameter of the electrode; lastly, ensure the method of manufacturing is practical, scalable and most importantly cost-effective for device mass-production and industrialisation.

9 – References

- ¹ J.R. Miller, A.F. Burke, *Electrochem. Soc. Interface* 17, 2008, 53.
- ² L.L. Zhang, X.S. Zhao, *Chem. Soc. Rev.* 38, 2009, 2520.
- ³ B.K. Kim, S. Sy, A. Yu, J. Zhang, *Handbook of Clean Energy Systems*, Wiley Online Library, 2015.
- ⁴ A.C. Dillon, *Chem. Rev.* 110, 2010, 6856.
- ⁵ Pod-Point Vehicle Guides: Nissan LEAF (2018); <https://pod-point.com/guides/vehicles/nissan/2018/leaf> ; accessed January 2021.
- ⁶ L.M. Da Silva, R. Cesar, C.M.R. Moreira, J.H.M. Santos, L.G. De Souza, B.M. Pires, R. Vicentini, W. Nunes, H. Zanin, *Energy Storage Materials* 27, 2020, 555.
- ⁷ B.D. Zdravkov, J.J. Čermák, M. Šefara, J. Janku, *Central European Journal of Chemistry* 5 (2), 2007, 385.
- ⁸ A.R. Koh, B. Hwang, K.C. Roh, K. Kim, *Phys. Chem. Chem. Phys.* 16, 2014, 15146.
- ⁹ J. Chmiola, G. Yushin, Y. Gogotsi, C. Portet, P. Simon, P.L. Taberna, *Science* 313 (5794), 2006, 1760.
- ¹⁰ J. Huang, B.G. Sumpter, V. Meunier, *Angew. Chem. Int. Ed.* 47 (3), 2008, 520.
- ¹¹ A. Slesinski, E. Frackowiak, *J. Solid State Electrochem* 22, 2018, 2135.
- ¹² L.M. Da Silva, L.A. De Faria, J.F.C. Boodts, *Electrochimica Acta* 47 (3), 2001, 395.
- ¹³ Y. Shao, M.F. El-Kady, J. Sun, Y. Li, Q. Zhang, M. Zhu, H. Wang, B. Dunn, R.B. Kaner, *Chemical Reviews* 118 (18), 2018, 9233.
- ¹⁴ F. Beguin, E. Frackowiak, (editors), *Supercapacitors: Materials, Systems, and Applications*. Weinheim: John Wiley & Sons, Incorporated; 2013.
- ¹⁵ R. Vicentini, L.M. Da Silva, E.P. Cecilio Junior, T.A. Alves, W.G. Nunes, H. Zanin, *Molecules* 24, 2019, 1452.
- ¹⁶ R. Vicentini, W.G. Nunes, L.H. Costa, A. Pascon, L.M. Da Silva, M. Baldan, H. Zanin, *IEEE Trans. Nanotechnol.* 18, 2019, 73.
- ¹⁷ Panasonic Industry Electric Double Layer Capacitors (Wound Type) Products Catalogue (2020); <https://industrial.panasonic.com/cdbs/www-data/pdf/RDH0000/DMH0000COL69.pdf>, pg. 8; accessed January 2021.
- ¹⁸ Maxwell Technologies: Cells: DuraBlue®, (2020); <https://www.maxwell.com/products/ultracapacitors/cells#20> ; accessed January 2021.
- ¹⁹ Aowei Technology: About Aowei (2018); <http://www.aowei.com/en/program/about-1.html> ; accessed January 2021.
- ²⁰ T. Hamilton, Next Stop: Ultracapacitor Buses, *MIT Technology Review* (2009); <https://www.technologyreview.com/2009/10/19/209306/next-stop-ultracapacitor-buses/> ; accessed January 2021.
- ²¹ B. Pal, S. Yang, S. Ramesh, V. Thangadurai, R. Jose, *Nanoscale Adv.* 1, 2019, 3807.
- ²² R. Kötz, M. Carlen, *Electrochimica Acta* 45, 2000, 2483.
- ²³ A.G. Pandolfo, A.F. Hollenkamp, *J. Power Sources* 157, 2006, 11.
- ²⁴ E. Frackowiak, F. Beguin, (editors), *Carbons for Electrochemical Energy Storage and Conversion Systems*. Baton Rouge: Taylor & Francis Group; 2009.
- ²⁵ X. Chen, R. Paul, L. Dai, *National Science Review* 4 (3), 2017, 453.
- ²⁶ D. Qu, *J. Power Sources* 109 (2), 2002, 403.
- ²⁷ C-T. Hsieh, H. Teng, *Carbon* 40 (5), 2002, 667.
- ²⁸ L. Bonnefoi, P. Simon, J.F. Fauvarque, C. Sarrazin, A. Dugast, *J. Power Sources* 79 (1), 1999, 37.
- ²⁹ M. Vijayakumar, R. Santhosh, J. Adduru, T.N. Rao, M. Karthik, *Carbon* 140, 2018, 465.
- ³⁰ B. Xu, F. Wu, R. Chen, G. Cao, S. Chen, Z. Zhou, Y. Yang, *Electrochem. Commun.* 10, 2008, 795.
- ³¹ P. Simon, Y. Gogotsi, *Nat. Mater.* 7, 2008, 845.
- ³² J.V. Alemán, A.V. Chadwick, J. He, M. Hess, K. Horie, R.G. Jones, P. Kratochvíl, I. Meisel, I. Mita, G. Moad, S. Penczek, R.F.T. Stepto, *Pure and Applied Chemistry* 79 (10), 2007, 1801.
- ³³ H. Pröbstle, M. Wiener, J. Fricke, *J. Porous Mater.* 10, 2003, 213.
- ³⁴ H. Pröbstle, C. Schmitt, J. Fricke, *J. Power Sources* 105, 2002, 189.
- ³⁵ Y.J. Lee, J.C. Jung, J. Yi, S.-H. Baeck, J.R. Yoon, I.K. Song, *Current Applied Physics* 10 (2), 2010, 682.
- ³⁶ W. Li, H. Pröbstle, J. Fricke, *J. Non-Cryst. Solids* 325, 2003, 1.
- ³⁷ T. Kyotani, Z. Ma, A. Tomita, *Carbon* 41 (7), 2003, 1451.
- ³⁸ T. Kyotani, *Prepr. Pap.-Am. Chem. Soc., Div. Fuel Chem.* 51 (1), 2006, 33.
- ³⁹ C.O. Ania, V. Khomenko, E. Raymundo-Pinero, J.B. Parra, F. Beguin, *Adv. Funct. Mater.* 17, 2007, 1828.
- ⁴⁰ D. Wang, F. Li, M. Liu, G.Q. Lu, H.-M. Cheng, *Angew. Chem. Int. Ed.* 47, 2008, 373.
- ⁴¹ A.C. Dillon, A.H. Mahan, P.A. Parilla, J.L. Alleman, M.J. Heben, K.M. Jones, K.E.H. Gilbert, *Nano Lett.* 3, 2003, 1425.

-
- ⁴² J.V.S. Moreira, E.J. Corat, P.W. May, L.D.R. Cardoso, P.A. Lelis, H. Zanin, *Journal of Electronic Materials* 45, 2016, 5781.
- ⁴³ E. Frackowiak, K. Jurewicz, K. Szostak, S. Delpeux, F. Beguin, *Fuel Process. Technol.* 77/78, 2002, 213.
- ⁴⁴ C. Niu, E.K. Sichel, R. Hoch, D. Moy, H. Tennent, *Appl. Phys. Lett.* 70, 1997, 1480.
- ⁴⁵ E. Frackowiak, S. Delpeux, K. Jurewicz, K. Szostak, D. Cazorla- Amoros, F. Beguin, *Chem. Phys. Lett.* 361, 2002, 35.
- ⁴⁶ K.H. An, W.S. Kim, Y.S. Park, J.-M. Moon, D.J. Bae, S.C. Lim, Y.S. Lee, Y.H. Lee, *Adv. Funct. Mater.* 11, 2001, 387.
- ⁴⁷ J.H. Chen, W.Z. Li, D.Z. Wang, S.X. Yang, J.G. Wen, Z.F. Ren, *Carbon* 40, 2002, 1193.
- ⁴⁸ D.N. Futaba, K. Hata, T. Yamada, T. Hiraoka, Y. Hayamizu, Y. Kakudate, O. Tanaike, H. Hatori, M. Yumura, S. Iijima, *Nature Materials* 5, 2006, 987.
- ⁴⁹ C. Liu, Z. Yu, D. Neff, A. Zhamu, B.Z. Jang, *Nano Lett.* 10, 2010, 4863.
- ⁵⁰ P.W. May, *Endeavour* 19 (3), 1995, 101.
- ⁵¹ K. Muzyka, J. Sun, T.H. Fereja, Y. Lan, W. Zhang, G. Xu, *Anal. Methods* 11, 2019, 397.
- ⁵² K.E. Bennet, K.H. Lee, J.N. Kruchowski, S.-Y. Chang, M.P. Marsh, A.A. Van Orsow, A. Paez, F.S. Manciu, *Materials* 6, 2013, 5726
- ⁵³ F. Gao, C.E. Nebel, *ACS Appl. Mater. Interfaces* 8, 2016, 28244.
- ⁵⁴ H. Masuda, M. Watanabe, K. Yasui, D. Tryk, T. Rao, A. Fujishima, *Adv. Mater.* 12 (6), 2000, 444.
- ⁵⁵ M. Yoshimura, K. Honda, R. Uchikado, T. Kondo, T.N. Rao, D.A. Tryk, A. Fujishima, Y. Sakamoto, K. Yasui, H. Masuda, *Diamond Relat. Mater.* 10, 2001, 620.
- ⁵⁶ J.V.S. Moreira, P.W. May, E.J. Corat, A.C. Peterlevitz, R.A. Pinheiro, H. Zanin, *J. Electron. Mater.* 46 (2), 2017, 929.
- ⁵⁷ X. Wang, Y. He, Z. Guo, H. Huang, P. Zhang, H. Lin, *New J. Chem.* 43, 2019, 18813.
- ⁵⁸ S. Yu, N. Yang, H. Zhuang, J. Meyer, S. Mandal, O.A. Williams, I. Lilge, H. Schönherr, X Jiang, *J. Phys. Chem. C* 119, 2015, 18918.